Modelling of tolerance and rebound in normal and diseased rats

Christine Ahlström

UNIVERSITY OF GOTHENBURG

Thesis for the degree of Doctor of Medicine

Modelling of tolerance and rebound
in normal and diseased rats

Christine Ahlström

Abstract

The development of rebound and tolerance is an important consideration when optimizing medical therapy, both with respect to drug dosing and adverse effects. By using quantitative approaches to study these processes, potential risks can be minimized. In this thesis nicotinic acid (NiAc)-induced changes in non-esterified fatty acids (NEFA) were used as a tool to investigate key determinants of tolerance and rebound in normal Sprague Dawley and in obese Zucker rats, a disease model of dyslipidaemia. The aim of the studies was to develop and challenge a model that described tolerance and rebound following different durations, rates and routes of NiAc administration.

In normal rats, administration of NiAc resulted in a rapid decrease in NEFA plasma concentration, followed by rebound, the extent of which depended on both the level and duration of drug exposure. Rebound oscillations followed long duration of NiAc exposure. During constant drug exposure, increasing NEFA concentrations indicated tolerance development. The pharmacodynamic characteristics of NiAc-induced changes in NEFA differed in normal and diseased rats, with NEFA baseline concentrations being increased, rebound diminished, and tolerance development more pro-nounced in the diseased animals.

The non-intuitive pattern of NiAc-induced changes in NEFA was captured by a feedback model with a moderator distributed over a series of transit compartments, where the first compartment inhibited the formation of response and the last stimulated the loss of response. The model was based on mechanistic principles, mimicking the dual actions of insulin in inhibiting the hydrolysis of triglycerides to NEFA and glycerol, and stimulating the re-esterification of NEFA. In both the normal and diseased rats, the model described the pharmacodynamic characteristics adequately.

The concentration-response relationship at steady state was shifted upwards and to the right, and was shallower, in diseased rats compared to normal rats. The extent of such shifts demonstrates the impact of disease at equilibrium in the system.

These studies have shown that by eliciting different exposure patterns and taking into account both the washout dynamics of the administered drug and the pharmacodynamic characteristics of normal and diseased animals, a mechanistically-based feedback model was able to tease out important information about tolerance and rebound.

List of publications

This thesis is based on the following publications, referred to in the text by the corresponding Roman numerals:

I   **Turnover modeling of non-esterified fatty acids in rats after multiple intravenous infusions of nicotinic acid**
Isaksson C., Wallenius K., Peletier LA., Toreson H., and Gabrielsson J.
Dose-Response **2009**, 7: 247-269

II   **Feedback modeling of non-esterified fatty acids in rats after nicotinic acid infusions**
Ahlström C., Peletier LA., Jansson-Löfmark R., and Gabrielsson J.
Journal of Pharmacokinetics and Pharmacodynamics **2011**, 38: 1-24

III   **Quantitative analysis of rate and extent of tolerance of biomarkers: Application to nicotinic acid-induced changes in non-esterified fatty acids in rats**
Ahlström C., Peletier LA., and Gabrielsson J.
Submitted to European Journal of Pharmaceutical Sciences **2011**

IV   **Challenges of a mechanistic feedback model describing nicotinic acid-induced changes in non-esterified fatty acids in rats**
Ahlström C., Peletier LA., and Gabrielsson J.
In manuscript

V   **Feedback modeling of non-esterified fatty acids in obese Zucker rats after nicotinic acid infusions**
Ahlström C., Peletier LA., and Gabrielsson J.
In manuscript

List of abbreviations

Pharmacokinetic and pharmacodynamic parameters and functions

A_b Amount of drug in biophase (µmol)

A_1 Linear absorption process

A_2 Nonlinear absorption process

A_g Amount of drug in gut (µmol)

AUC_E Area under the positive effect time-course (mmol·min·L^{-1})

AUC_R Area under the rebound time-course (mmol·min·L^{-1})

BW Body weight

C_p Drug plasma concentration (µmol·L^{-1})

C_{SS} Drug concentration at steady state (µmol·L^{-1})

C_t Drug peripheral concentration (µmol·L^{-1})

Cl_d Intercompartmental distribution (L·min^{-1}·kg^{-1})

Cl_{tot} Total clearance (L·min^{-1}·kg^{-1})

$Dose_{po}$ Oral dose of NiAc (µmol·kg^{-1})

$f(R)$ Feedback function dependent on the response R

f_u Fraction unbound (%)

$H(C_p)$ Drug mechanism function. See also $I(C_p)$

$I(A_b)$ Inhibitory drug mechanism function driven by A_b

IC_{50} Concentration in plasma reducing k_{in} by 50 % (µmol·L^{-1})

$I(C_p)$ Inhibitory drug mechanism function driven by C_p

ID_{50} Amount in biophase reducing k_{in} by 50 % (µmol)

I_{max} Maximum drug-induced inhibition

Inf Exogenous NiAc infusion rate (µmol·min^{-1}·kg^{-1})

$Input$ Exogenous NiAc input rate (µmol·min^{-1} kg^{-1})

k_a First-order absorption rate constants (min^{-1})

k_{cap} Formation of NEFA in capillaries (mmol·L^{-1}·min^{-1})

k_e Elimination rate constant (min^{-1})

k_{in} Turnover rate for production of response (mmol^2·L^{-2}·min^{-1})

K_{m1} Michaelis-Menten constant, high affinity pathway 1 (µmol·L^{-1})

K_{m2} Michaelis-Menten constant, low affinity pathway 2 (µmol·L^{-1})

$K_{m,g}$ Amount of drug in gut at half max. absorption rate (µmol·kg^{-1})

k_{out} Fractional turnover rate of response (L·mmol^{-1}·min^{-1})

k_{tol} Turnover rate constant of moderator (min^{-1})

M Moderator (mmol·L^{-1})

M_i Moderator in compartment i where i = 1, ..., 8 (mmol·L^{-1})

M_N Moderator in compartment N (mmol·L^{-1})

N	Number of moderator transit compartments
p	Amplification factor of impact of M_1 on k_{in}
P	Pool/precursor to the response
PKPD	Pharmacokinetic-pharmacodynamic
R	NEFA plasma concentration (response) (mmol·L^{-1})
R_0	Baseline NEFA plasma concentration (mmol·L^{-1})
R_{min}	Lowest measured response (mmol·L^{-1})
R_{SS}	Pharmacodynamic steady state NEFA concentration (mmol·L^{-1})
$Synt$	Endogenous NiAc synthesis rate (μmol·min^{-1}·kg^{-1})
$t_{1/2}$	Half-life (min)
V_c	Central volume of distribution (L·kg^{-1})
V_{max1}	Maximal velocity, high affinity pathway 1 (μmol·min^{-1}·kg^{-1})
V_{max2}	Maximal velocity, low affinity pathway 2 (μmol·min^{-1}·kg^{-1})
$V_{max,g}$	Maximal absorption rate (μmol·min^{-1}·kg^{-1})
V_t	Peripheral volume of distribution (L·kg^{-1})
γ	Sigmoidicity factor

Abbreviations of the analysis

CV %	Precision of parameter estimate calculated as (SE/mean)·100
HPLC	High performance liquid chromatography
IIV	Inter-individual variability (%)
LC-MS	Liquid chromatography mass spectrometry
LLOQ	Lower limit of quantification
OFV	Objective function value
RSE	Relative standard error (%)
SE	Standard error
σ	Residual proportional (σ_1, %) or additive (σ_2) error

Biomarkers

AC	Adenylyl cyclase
AMP	Adenosine monophosphate
ATP	Adenosine triphosphate
cAMP	cyclic AMP
HDL	High-density lipoprotein
HSL	Hormone-sensitive lipase
LDL	Low-density lipoprotein
NEFA	Non-esterified fatty acids
NiAc	Nicotinic acid
PKA	Protein kinase A
TG	Triglycerides
VLDL	Very-low-density lipoprotein

Table of contents

1   Introduction

1.1   Background

Pharmacokinetics describes the absorption, distribution, metabolism and excretion of a drug whereas pharmacodynamics represents the relationship between drug concentration and the onset, intensity and duration of a pharmacological response [1, 2]. Pharmacodynamics includes the exploration and assessment of relevant variables such as pharmacologically active metabolites, functional adaptation and the effects of genetics and of underlying diseases [3]. A pharmacokinetic-pharmacodynamic (PKPD) model can be used to summarize quantitatively knowledge about the mechanism of drug action, the pharmacokinetic and pharmacological properties of the drug, and the impact of disease on the pharmacological response.

Exposure of intended targets or receptors to a drug over an extended period of time may cause a progressive reduction in the response to the drug. This phenomenon is variously termed desensitization, tachyphylaxis, functional adaptation, or tolerance. The extent of tolerance and rebound varies with the type of drug, probably reflecting diversity in the basic mechanism of tolerance and rebound development [4]. Although many researchers have investigated tolerance and rebound [*e.g.* 5-11], there is need for a broader understanding of quantitative aspects of the rate and extent of development of tolerance and rebound. In the studies underpinning this thesis nicotinic acid (NiAc)-induced changes in non-esterified fatty acids (NEFA) were used as a tool to study key determinants of rate and extent of tolerance and rebound in normal and diseased rats.

NiAc is used as a treatment for dyslipidaemia and has been associated with a decrease in cardiovascular events such as myocardial infarction and death [12-14]. NiAc inhibits lipolysis in adipose tissue, resulting in a pronounced decrease in plasma NEFA concentrations [15, 16]. Although NiAc has been used clinically for years, its pharmacokinetic and pharmacodynamic properties, including tolerance and rebound, are not fully understood.

It is known that a rapid decrease in exposure to a drug may enhance rebound, and a gradual decline may confound it [17-22]. Furthermore, when there is rapid pharmacokinetics, the turnover of the pharmacodynamic system becomes the rate limiting step and rebound may become evident. In the case of NiAc, elimination is rapid and a NiAc-induced reduction in NEFA concentrations is seen within a few minutes of onset of treatment. This, together with the short half-life of NiAc implies that informative experiments for studying tolerance and rebound can be performed within a few hours of drug administration.

Although it is known that binding of drugs to other receptors such as adenosine receptors also reduces NEFA plasma concentrations [23, 24], the regulation of these processes is intentionally not addressed here, as setting up a general model of NEFA regulation to include all major endogenous determinants was beyond the scope of the investigations.

1.2   Dyslipidaemia
Dyslipidaemia is diagnosed as an abnormal concentration of one or more plasma lipoproteins. Common biomarkers of dyslipidaemia include elevated levels of total cholesterol, low-density lipoprotein (LDL) cholesterol and tri-glycerides (TG), and low levels of high-density lipoprotein (HDL) cholesterol, all of which can occur in isolation or in combination [25]. Elevated levels of total cholesterol, LDL cholesterol and TG, and low levels of HDL cholesterol are major risk factors for coronary heart disease and other forms of atheros-clerotic vascular diseases [26]. In 2004, 7.2 million people died globally from coronary heart disease, and 5.7 million from stroke [27].

1.3   Nicotinic acid
As a clinical treatment for dyslipidaemia, oral doses of 1-3 grams of NiAc per day lower total cholesterol, LDL cholesterol, very-low-density lipoprotein (VLDL) cholesterol and plasma TG, and simultaneously raise HDL cholesterol (HDL) [28-35]. NiAc has been shown to reduce the risk of recurrent myo-cardial infarction [36] and the mortality from coronary heart disease in man [12-14, 37]. These benefits probably result from the ability of NiAc to inhibit lipolysis in adipose tissue and thereby reduce plasma NEFA concentrations [16].

Conceptually, the antilipolytic effect of NiAc might provide a way to improve glucose tolerance in pre-diabetic or diabetic patients. Indeed, several reports indicate that NiAc or its analogues improve glucose use and insulin sensitivity

in type 2 diabetic patients, at least in the short term [38-40]. This is in contrast to reports indicating that the long-term administration of NiAc decreases glucose tolerance in these patients [41]. A NiAc analogue that, taken prior to a meal, rapidly decreases NEFA concentrations substantially with short effect duration (*e.g.* around 2 h) and no rebound might be a compound to aim for. With reduced NEFA concentration, glucose will be used as a source of energy, which may result in improved insulin sensitivity. Short effect duration has proven to be beneficial for systems exhibiting tolerance, as the primary effect does not last long enough for the counter-acting mechanisms, accountable for tolerance and rebound, to develop [42-47].

The lipid-lowering effect of NiAc was discovered by Altschul *et al.* in 1955 [48]. However, the mechanism of action was not clarified until 2003 when several groups reported that the G protein-coupled receptor GPR109A (HM74A in humans; PUMA-G in mice) is activated by NiAc concentrations elicited by therapeutic doses [49-51]. When NiAc binds to the receptor in adipose tissue, a cascade of events commences, resulting in inhibited hydrolysis of TG to NEFA and glycerol (Figure 1). Consequently, the release of NEFA to the circulation is reduced, which results in a substrate shortage for liver synthesis and secretion of TG and VLDL, which eventually leads to a decrease of VLDL, LDL, and TG levels in plasma [15, 16, 52-54]. However, the mechanism of the nicotinic acid-induced increase of HDL levels in plasma is still not known [55, 56].

Although NiAc is efficacious and favourably modifies the lipoprotein profile, its long-term use is limited for many patients because of its adverse effects, including flushing and itching of the skin, gastrointestinal distress, glucose intolerance, hepatotoxicity, hyperuricaemia, and other rarer side effects [57]. Furthermore, the time-course of NiAc-induced changes in plasma NEFA concentrations is complex, including tolerance and rebound. To increase the probability of finding a drug that affects the same pathway but exhibits less tolerance and rebound, the NiAc-induced pattern of NEFA response needs to be characterized quantitatively to further understand its homeostatic control mechanisms and its exposure-response relationship in normal and diseased animals. These factors can then be used when predicting the onset, intensity and duration of response following different drug exposure scenarios in humans, enabling the dose regimen to be optimized so as to minimize adverse effects.
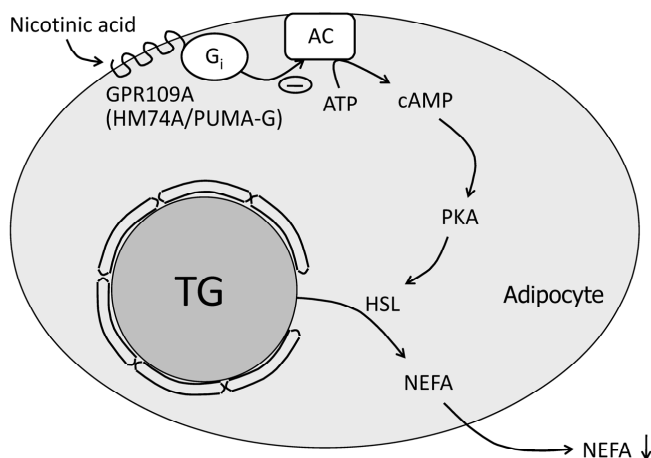
Figure 1. *Mechanism of NiAc-induced changes in lipid metabolism. Activation of the G protein-coupled receptor GPR109A by nicotinic acid (NiAc) results in inhibition of adenylyl cyclase (AC) activity, leading to decreased formation of cyclic adenosine monophosphate (cAMP) from adenosine triphosphate (ATP). cAMP regulates lipolysis in adipocytes by activating protein kinase A (PKA); in turn, PKA phosphorylates hormone-sensitive lipase (HSL). The hydrolysis of triglycerides (TG) into non-esterified fatty acids (NEFA) and glycerol, which is catalyzed by HSL, is thus reduced by NiAc. Adapted from Offermanns, 2006* [58].

1.4 Tolerance and rebound

1.4.1 Mechanisms behind development of tolerance

A broad definition of tolerance is "a pharmacologically defined phenomenon that appears after one or several exposures to a drug, when the same dose or concentration of the same drug produces a smaller response than that which appears in appropriate controls" [59]. When tolerance occurs after one dose of the drug or within the duration of one continuous drug exposure, it is called acute tolerance or tachyphylaxis [4]. The development of tolerance to drug action is an important consideration in optimizing medical therapy, both with respect to drug dosing and adverse effects, and it can be characterized quantitatively using PKPD models. These models are useful when designing dosing regimens and, by providing mechanistic information about drug action, may assist in finding ways of influencing the development of tolerance [60].

Mechanistically, tolerance may be categorized as 1) dispositional or pharmacokinetic, 2) functional or pharmacodynamic, 3) behavioural, or

4) conditioned [60]. Dispositional (pharmacokinetic) tolerance occurs when repeated doses or sustained exposure to a drug result in increased metabolism [4]. In functional (pharmacodynamic) tolerance, the response to a given concentration of the drug at the receptor site or another site of action is altered over time [4]. Behavioural tolerance, which accompanies some psychoactive drugs, is evidenced as learning to compensate for the effect of the drug on a particular skill [61, 62]. Conditioned tolerance develops to exposure in one particular environment, but not necessarily in another environment [63-65]. The studies reported in this thesis focus on functional tolerance.

Functional tolerance may be due to 1) changes in post-receptor regulation such as depletion of an endogenous intermediary (*e.g.* a neurotransmitter); 2) inactivation or reduction (down-regulation) in numbers of receptors; or 3) development of homeostatic feedback mechanisms [66] (Figure 2).

1.4.2 Mechanisms behind development of rebound

Rebound is the characteristics of a drug to produce contrary effects when the effect of the drug has passed or the patient no longer responds to it. There are many different classes of medication, as well as specific drugs, which produce rebound, including antidepressants [67-71], opioides [72, 73], beta-adrenoceptor blockers [74, 75] and nitroglycerine [20, 76-79].

In most cases, the rebound effect occurs after regular use of a medication (*i.e.* once or twice weekly, to daily, usage) followed by abrupt discontinuation, but rebound may also appear after a single drug dose. Rebound becomes a safety problem if the response has the potential to be toxic or life-threatening. For this reason, rebound is unwanted. With gradual drug withdrawal it may be possible to reduce the magnitude of the rebound [18, 20, 22].

After a drug is taken, endogenous counteracting mechanisms may pull in the opposite direction to the drug as they try to return the body to its pre-existing state [80]. These counteracting mechanisms are often seen as developing tolerance during drug treatment.

If the regulation of the counteracting mechanisms is slow in comparison to the decline of drug effect it may outlast the drug effect, leading to rebound [20, 81].

Termination of treatment with an antagonist may give rise to a rebound effect because, after prolonged contact with antagonist, new receptors may have been formed (up-regulation), leading to increased tissue sensitivity. As a result, the response to endogenous agonist may increase after washout of the antagonist. Up-regulation of receptors may be responsible for rebound hypertension, appearance of angina pectoris or increased heart rate following withdrawal of beta-adrenoceptor blockers [82, 83].
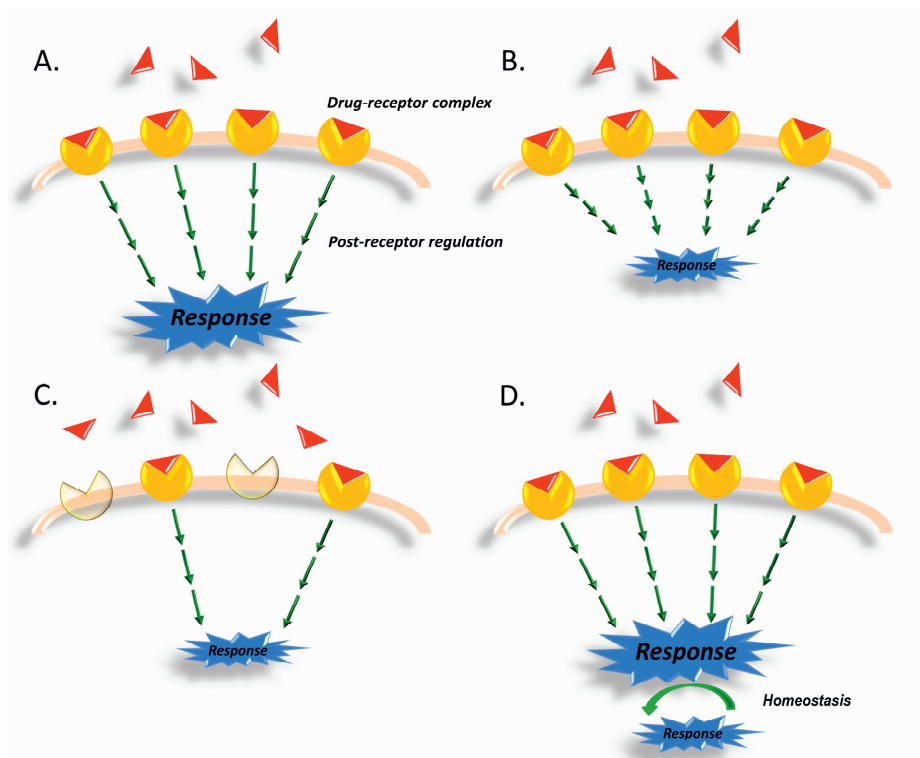
Figure 2. Schematic illustrations of basic events leading to a pharmacological response following drug administration (A), and of mechanisms underlying functional tolerance (B-D). The red triangles and yellow circles represent the drug and receptor, respectively. (A) Interaction of a drug with its receptor produces a drug-receptor complex, which directly or indirectly regulates some function (post-receptor regulation), detected as the drug-induced response. (B) Tolerance caused by changes in post-receptor regulation such as depletion of an intermediary. (C) Tolerance resulting from receptor inactivation or down-regulation. (D) Tolerance consequent on developing homeostatic feedback mechanisms which counteract the primary response. Adapted from Gabrielsson and Weiner, 2006 [84].

1.4.3 Experimental designs for studying tolerance and rebound

As it may be difficult to detect tolerance following a single dose of drug, other dosing regimens may be needed to reveal it. One approach is the use of repeated doses of a drug at varying time intervals. When a second dose is administered in close temporal proximity to a previous dose, the magnitude of the second response will be smaller if there is any tolerance. If sufficient time is allowed between doses, tolerance will dissipate, and the two responses will be similar [47, 85-89]. Another approach involves giving a constant infusion of drug to achieve and maintain a relatively constant plasma concentration over a prolonged period of time. A decline in response in spite of constant drug exposure indicates development of functional tolerance [46, 87, 89-93].

An important factor determining the size of rebound is the decline in exposure of test compound in relation to the turnover rates of the physio-logical system. Rapid decline in exposure tends to cause a large rebound, whilst gradual decline tends to confound rebound [17-22]. In order to characterize the rate and extent of rebound, the pharmacodynamic response must be sampled throughout washout.

1.5 Modelling of tolerance and rebound

1.5.1 Introduction to PKPD modelling

Mathematical models can be fitted to experimental data to describe the time-course of drug exposure and response using linear or nonlinear regression methods [1, 2, 94, 95]. The most common approach involves sequential analysis of plasma concentration *versus* time data, followed by response *versus* time data, with the plasma kinetic model providing an input function that drives the response of some biomarker [1]. However, high quality pharmacodynamic data, even in the absence of measured drug concentrations, contain information about a drug's biophase kinetics which can be used to drive and quantify the response [96]. This approach is referred to as dose-response-time analysis.

Ideally, a model should be mechanistically based as this facilitates extra-polation to other experimental conditions. A key element of such modelling is the explicit distinction between parameters for describing drug-specific properties and biological system-specific properties. Mechanism-based PKPD models contain specific expressions for the characterization of processes between drug exposure and biomarker response such as target-site

distribution, target binding and activation, biomarker turnover, time-dependent transduction mechanisms, homeostatic feedback mechanisms, disease processes, and disease progression [97]. By changing the drug-specific components of a model to those of another drug, it is possible to predict the consequences of different drug treatments. Thus, a mechanistic model has the potential to be predictive beyond the range of data upon which it was developed. Furthermore, mechanistic models enable different sources of information to be merged into one model, so that underlying functional mechanisms may be better understood.

1.5.2 Categories of tolerance and feedback models

In the past, there have been several approaches to modelling tolerance and feedback, including models based on a single turnover equation (Figure 3A) [98-100], pool/precursor models (Figure 3B) [81, 101, 102], and models that include moderator-induced negative feedback (Figure 3C) [22, 103-107]. In addition, tolerance has been modelled as formation of a hypothetical metabolite which acts as an antagonist to the positive effect of the parent compound [47, 88] and as time-dependent attenuation of parameters resulting in *e.g.* decreased efficacy or potency of the drug over time [108, 109].

In tolerance models based on a single turnover equation (Figure 3A), turnover rate is governed by the level of response. When the response approaches a physiological limit, the turnover rate is reduced. These models do not capture rebound or overshoot. In pool/precursor models (Figure 3B), a pool P is respectively produced and lost by means of k_{in} and k_{tol}, with the mass of the pool then providing input to the response compartment R. The loss from the pool may be stimulated or inhibited by the drug, represented by $H(C_p)$. If a certain fraction of the pool is pushed into the response compartment R, resulting in a positive effect area above the baseline (AUC_E), an equal fraction will be needed to refill the pool before the original equilibrium can be re-established. The period of refill results in a response below the baseline, also called the rebound. The area of the rebound AUC_R, equals the area of the positive response AUC_E. This is a phenomenon seldom seen in biological systems.

In feedback models, the feedback may be represented by an endogenous moderator M that counteracts changes in the response R (Figure 3C). A drug-induced increase in R results in an increase in M that feeds back and affects the level of R negatively. With slow moderator dynamics (*e.g.* k_{tol} is small relative to k_{out}) R will overshoot before it settles at the pharmacodynamic

steady state R_{SS}. If the drug stimulus is quickly removed, the delayed counteracting effect of M will result in rebound. For these models, the positive effect area AUC_E before the original equilibrium is re-established is generally different from AUC_R. These models have proven to be flexible for characterizing the onset, intensity and duration of a response in systems that exhibit feedback, tolerance and rebound [22]. In the studies described in this thesis, the feedback model in Figure 3C has been adjusted and extended to describe NiAc-induced changes in turnover of NEFA.
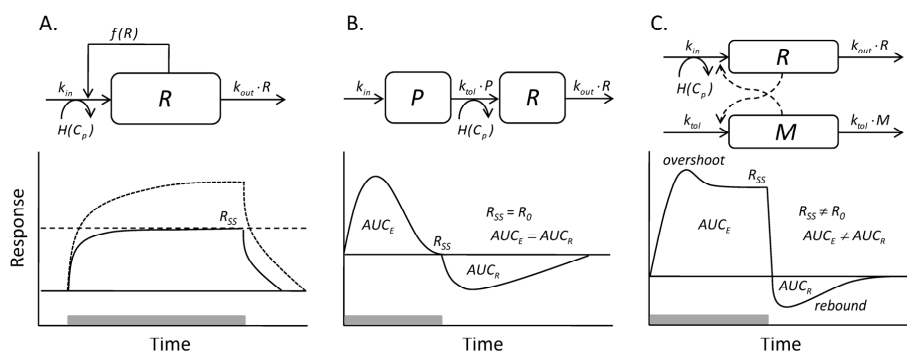

Figure 3. *Schematic illustrations of three categories of tolerance models (upper panels) and their response-time profiles during and after drug infusion (lower panels). The grey bars represent the period of drug infusion. (A) Simple feedback affecting turnover rate; (B) pool/precursor model; and (C) negative feedback via a moderator. R represents the measured response, P a precursor, M an endogenous moderator, k_{in} the turnover rate constant for production of R, and k_{out} and k_{tol} the first-order rate constants for loss of R, and for loss of P plus production and loss of M, respectively. $H(C_p)$ indicates the site where drug must act to elicit tolerance/rebound in the R compartment. AUC_E and AUC_R represent the positive effect and rebound area, respectively, and R_0 and R_{SS} the baseline and steady state response, respectively. The dashed line in (A) represents the physiological limit of the response, and the dashed curve the response without tolerance. Although not shown in (A), the loss term $k_{out}\cdot R$ may also provide simple feedback.*

1.6 PKPD modelling in diseased states

There are many reasons for large inter-individual variability in the pharmaco-dynamics of drugs, one of which is the presence of underlying disease [3, 110-117]. However, in the clinic it is often difficult to establish whether a disease-associated change in the temporal pharmacological profile of a drug is of purely pharmacokinetic or pharmacodynamic origin. This is further complicated by the unstable nature of most diseases and by the fact that few patients suffer from only one well-defined disease. Therefore, studies of the

kinetics of drug action in diseased states in animal models under well-defined conditions are crucial [110].

Dyslipidaemia is frequently associated with obesity and insulin resistance. Obesity may influence the distribution and clearance of compounds [118-123]. Insulin is known to influence the regulation of NEFA turnover in healthy individuals by inhibiting the hydrolysis of TG to NEFA and glycerol [124, 125] and by stimulating the re-esterification of NEFA to TG [125, 126]. It is therefore possible that NEFA homeostasis is altered in patients suffering from obesity and insulin resistance. Disease-induced hormonal changes may also affect NEFA turnover. Consequently, the onset, intensity and duration of drug effects may change. Therefore, the impact of disease on the structural PKPD model, system parameters, drug parameters and pharmacokinetics need to be assessed as a part of the model building process.

2 Aims and progression of studies

The studies described in this thesis were undertaken to investigate the key determinants of tolerance and rebound in normal and diseased rats. To achieve this, nicotinic acid (NiAc)-induced changes in non-esterified fatty acids (NEFA) were used as a tool-system.

2.1 Specific aims
The specific aims were:

- To develop a dose-response-time feedback model describing NiAc-induced changes in NEFA plasma concentrations in the absence of measurements of NiAc exposure in normal rats (Paper I), and to use that information for subsequent experimental design

- To develop and challenge a feedback model that describes the tolerance and oscillatory rebound of NEFA plasma concentrations following different durations, rates and routes of NiAc administration to normal rats (Papers II and IV)

- To evaluate the major determinants of rate and extent of tolerance and rebound found in normal rats by means of a mathematical/analytical and numerical approach (Paper III)

- To develop a model that describes NEFA plasma concentrations following NiAc infusions in an animal model of dyslipidaemia, in order to evaluate the impact of disease on the NiAc-induced changes in NEFA turnover (Paper V)

2.2 Progression of studies

The results described in these studies were based on a feedback model in which the feedback is described by means of an endogenous moderator *M* that counteracts changes in the response *R* (*i.e.* in NEFA formation). This model has previously been published by Ackerman [103], Wakelkamp *et al.* [104], Zuideveld *et al.* [105], Bundgaard *et al.* [106], and Gabrielsson and Peletier [22, 107]. Because the model had been shown to adequately describe NiAc-induced changes in NEFA response in normal rats in the absence of measured NiAc exposure (dose-response-time analysis, Paper I), it was used here to simulate new experiments.

In the rat experiments described in Paper II, which were designed based on the model in Paper I, the response-time data elicited by different infusion regimens revealed a lower physiological limit in NEFA response, slowly developing tolerance in spite of constant drug exposure, and oscillations in the rebound primarily following long infusions. Because the model used for the dose-response-time analysis in Paper I failed to capture these characteristics, it was extended in Paper II to include a series of moderator compartments to capture the feedback. In this new model, the first moderator inhibited the formation of response, and the last stimulated the loss of response. With these changes, the characteristics of the NEFA response in normal rats were captured successfully. Mechanistically this may represent the dual actions of insulin on NEFA regulation [124-126].

In order to understand why this new model succeeded where the initial model had failed, it was analyzed mathematically in Paper III, focussing primarily on the rate and extent of tolerance and rebound.

The model was then challenged in new experiments in Paper IV, with NiAc being administered to normal rats at different rates and by different routes, resulting in diverse exposure patterns. The new model described the NEFA response following these provocations adequately.

In Paper V, the model was challenged further, with its applicability being tested to pharmacodynamic data obtained from rats with dyslipidaemia. It was found to describe the altered characteristics of the animals both at baseline and following administration of NiAc.

3   Materials and methods

3.1   Animals

Male Sprague Dawley rats (Harlan Laboratories B.V., The Netherlands), weighing 220-447 g, were used in Papers I, II and IV. In Paper V, male Zucker rats [127-129](Harlan Laboratories B.V., The Netherlands), weighing 473-547 g, were used. All rats were housed and acclimatized in groups of 2-6 for at least one week prior to surgery. The studies were approved by the Ethics Committee for Animal Experiments, Gothenburg, Sweden. Animals were kept in climate-controlled facilities at a room temperature of 20–22 °C and relative humidity of 40–60 % under a 12:12-h light:dark cycle (lights on at 6:00 am) and standard diet and tap water were available *ad libitum*.

3.2   Surgical procedure

The rats in Paper I were anaesthetized with an intra-peritoneal injection (180 mg·kg^{-1} BW) of Na-thiobutabarbital (Inactin®, Sigma Chemical Co., St Louis, MO, USA) and tracheotomized with PE 240 tubing (Intramedic®, Becton Dickinson and Company, USA). One catheter (PE 50 tubing; Intramedic®, Becton Dickinson and Company, USA) was placed in the left carotid artery for blood sampling and recording of arterial blood pressure. Two catheters (PE 10 tubing; Intramedic®, Becton Dickinson and Company, USA) were inserted into the right jugular vein, one for infusion of NiAc or vehicle and the other for infusion of diluted Na-thiobutabarbital. The animals were allowed a minimum post-surgical recovery period of 1.5 h to enable glucose levels to stabilize.

The rat surgery in Papers II, IV and V was performed under isoflurane (Forene®, Abbott Scandinavia AB, Solna, Sweden) anaesthesia. One catheter was implanted in the left carotid artery (PE 25 tubing; Intramedic®, Becton Dickinson and Company, USA) for blood sampling, and one in the right external jugular vein (PE 50 tubing; Intramedic®, Becton Dickinson and Company, USA) for drug administration. After cannulation, the catheters

were exteriorized at the nape of the neck and sealed. After surgery, the rats were housed individually and allowed a minimum of 5 days to recover. In all studies a sterile sodium-citrate solution (20.6 mM Na_3-citrate in sterile saline; Pharmaceutical and Analytical R&D, AstraZeneca, Mölndal, Sweden) was used to prevent clotting in the catheters.

3.3 Experimental design

3.4.1 Paper I

Paper I was an inventory of previous performed experiments that were originally designed to qualitatively assess the behaviour of plasma NEFA concentrations after different NiAc provocations, rather than for a quantitative PKPD analysis. As a result, the exposure to NiAc was not characterized, and sampling schedule was intended to detect the maximum and minimum response to NiAc and to demonstrate rebound. The data collected were therefore more exploratory than optimal in the context of parameter identification.

NiAc, dissolved in sterile 0.9 % NaCl, was administered as intravenous infusions to anaesthetized rats using four different infusion regimens (Table 1). The concentrations of the dosing solutions were adjusted to give infusion flow rates in the range of 0.7-40 µL·min^{-1}. Arterial blood samples (13-24 per rat, 30 µl per sample) were collected predose and during the infusion and washout periods for analysis of NEFA. The total blood volume removed did not exceed 0.8 mL.

Table 1. Experimental design for Paper I (normal Sprague Dawley rats)

Dosing regimen	Study 1 n=10[*]	Study 2 n=1	Study 3 n=1	Study 4 n=1
Infusion	Consecutive infusions	Single infusion	Consecutive infusions	Progressive plus constant rate infusions
Rate (nmol·min^{-1})	0.8, 1.6, 3.2, 6.4, 12.8, 25.6	26	32, 64	0→13[**], 13, 13→0[**]
Duration (min)	30, 30, 30, 30, 30, 40	30	73, 31	30, 30, 30
Total dose (mg·kg^{-1})	0, 0.5	0.2	1	0.2

[*] n=7 in the treatment group and n=3 in the control group; control rats received vehicle for the same total duration as treated rats
[**] 3 min stepwise rate changes

3.4.2 Paper II

The aim of Paper II was to assess the NiAc-induced changes in NEFA from a quantitative point of view using normal Sprague Dawley rats. Animals were assigned to 8 groups, each of which received an intravenous constant rate infusion for either 30 or 300 min (Table 2). Four groups received vehicle (0.9 % NaCl, n = 10), or 1, 5 or 20 µmol·kg^{-1} NiAc (n = 4-9 per group) over 30 min. The other 4 groups received vehicle (n = 8), or 5, 10 or 51 µmol·kg^{-1} NiAc (n = 7-9 per group) over 300 min.

Table 2. *Experimental design for Papers II and IV (normal Sprague Dawley rats)*

Dosing regimen	Dose (µmol·kg^{-1})	Rate (µmol·min^{-1}·kg^{-1})	Length of infusion (min)	Number of rats	Paper
Infusion	0	0[*]	30	10	II, IV
	1	0.033		4	
	5	0.17		8	
	20	0.67		9	
	0	0[*]	300	8	
	5	0.017		9	
	10	0.033		8	
	51	0.17		7	
	0	0, 0[*]	30, 180[*]	1	IV
	5, 5→0.033[**]	0.17, 0.17→0.0033[**]	30, 180[**]	5	
	0	0, 0, 0[*]	30, 180[*], 30	1	
	5, 5→0.033[**], 5	0.17, 0.17→0.0033[**], 0.17	30, 180[**], 30	5	
Oral	0	-	-	6	IV
	24.4	-	-	6	
	81.2	-	-	6	
	812	-	-	6	

[*] Control rats received vehicle using the same dose regimen as the NiAc group

[**] Stepwise decrease in dose of 0.009 µmol·min^{-1}·kg^{-1} every 10 min

The concentrations of the dosing solutions were adjusted to give infusion volume flow rates in the range of 3.5-22 µL·min^{-1}, based on body weight. The dosing solutions were prepared within 30 min of administration by dissolving an appropriate amount of NiAc in saline solution. Multiple (11-13 per rat) arterial blood samples were drawn for analysis of NiAc and NEFA plasma

concentrations. The total volume of blood removed did not exceed 1.5 mL per animal.

3.4.3 Paper III

The feedback model developed to describe NiAc-NEFA data in Paper II was evaluated from a mathematical/analytical perspective, focussing on the rate and extent of tolerance and rebound development. Numerical simulations were done to further explore the model behaviour.

3.4.4 Paper IV

In Paper IV, the data set from Paper II was extended using different intravenous and oral dosing regimens to produce additional patterns of NiAc exposure. This was done to explore the NiAc-induced changes in NEFA under new conditions, and to challenge the model.

Each animal was assigned to one of 16 groups (Table 2). Groups 1-8 received an intravenous constant rate infusion of vehicle (0.9 % NaCl, n = 18) or NiAc (n = 4-9 per group) for either 30 or 300 min. NiAc infusions of 0, 1, 5 or 20 $\mu mol \cdot kg^{-1}$ body weight were given over 30 min, and of 0, 5, 10 or 51 $\mu mol \cdot kg^{-1}$ over 300 min. Group 10 received a total NiAc dose of 20 $\mu mol \cdot kg^{-1}$ administered as a constant infusion (5 $\mu mol \cdot kg^{-1}$, n = 5) for 30 min, followed by a stepwise decrease in infusion rate every 10 min for 180 min; the flow rate and treatment duration for vehicle in the control (group 9, n = 1) were the same as in group 10. Group 12 (n = 5) received a total NiAc dose of 25 $\mu mol \cdot kg^{-1}$ administered according to the same regimen as group 10 for the first 210 min; at which time a subsequent 30 min infusion of 5 $\mu mol \cdot kg^{-1}$ was given; its control (group 11, n = 1) received vehicle according to the same regimen. Groups 13-16 were dosed orally by gavage with vehicle or 24.4, 81.2, or 812 $\mu mol \cdot kg^{-1}$ NiAc (n = 6 per group). The concentrations of the dosing solutions were adjusted to give infusion volume flow rates in the range 0.4-22 $\mu L \cdot min^{-1}$ and an oral dosing volume in the range 1.4-1.6 mL, based on body weight. All dosing solutions were prepared within 30 min of administration by dissolving NiAc in saline. Multiple (11-15 per rat) arterial blood samples were drawn for analysis of NiAc and NEFA plasma concentrations. The total volume of blood removed did not exceed 1.5 mL per animal.

3.4.5 Paper V

NiAc was administered to obese Zucker rats, an animal model of dyslipidaemia exhibiting insulin resistance and obesity [129], to assess the impact of disease on NiAc-induced changes in NEFA turnover. Animals were

assigned to 4 groups of rats each of which received an intravenous constant rate infusion for either 30 or 300 min (Table 3). Two groups received vehicle (0.9 % NaCl) or 20 µmol·kg^{-1} NiAc over 30 min, and 2 groups vehicle or 51 µmol·kg^{-1} NiAc over 300 min. The concentrations of the dosing solutions were adjusted to give infusion volume flow rates in the range 5.7-18 µL·min^{-1}. Multiple (13-14) arterial blood samples were drawn for analysis of NiAc and NEFA plasma concentrations. The total volume of blood removed did not exceed 1.5 mL per animal. Data from the obese rats were compared with comparable data from normal rats reported in Papers II and IV.

Table 3. *Experimental design for Paper V (obese Zucker rats)*

Dosing regimen	Dose (µmol·kg^{-1})	Rate (µmol·min^{-1}·kg^{-1})	Length of infusion (min)	Number of rats
Infusion	Control	0	30	2
	20	0.67		8
	Control	0	300	2
	51	0.17		7

* Control rats received vehicle using the same dose regimen as the NiAc group

3.4 Analytical assays

NiAc plasma concentration was analyzed and quantified using LC-MS. The high performance liquid chromatography (HPLC) system was an Agilent 1100 Series (Hewlett-Packard GmbH, Walbronn, Germany) coupled to an HTC PAL auto sampler (CTC Analytics AG, Zwingen, Germany). Plasma samples (50 µL per sample) were precipitated with cold acetonitrile containing 0.2 % formic acid (150 µL per sample). After vortex mixing and centrifugation at 4 °C (4 000 × g, 20 min), an aliquot of 100 µL of the supernatant was used for the analysis. The mobile phase consisted of (A) 2 % acetonitrile and 0.2 % formic acid in water and (B) 0.2 % formic acid in acetonitrile. Separation was performed on a 50 x 2.1 mm Biobasic AX column with 5 µm particles (Thermo Hypersil-Keystone, Runcorn, Cheshire, UK) with a gradient of 95 to 20 % B over 1 min, held at 20 % B for 1.5 min and returned to initial conditions in one step. The HPLC system was connected to a Sciex API 4000 quadrupole mass spectrometer with a positive electrospray ionization interface (Applied Biosystems, Ontario, Canada) and the mass transition was 124.0 > 80.2. Data acquisition and data evaluation were performed using Analyst 1.4.1 (Applied Biosystems). The method showed linearity over a concentration range of 0.001-250 µmol·L^{-1}. The lower limit of quantification (LLOQ) was 0.001 µmol·L^{-1} applying a sample volume of 50 µL plasma.

Plasma NEFA concentration was analyzed using an enzymatic colourimetric method (Wako Chemicals GmbH, Neuss, Germany) adapted to a 96-well format. This method relies upon the acylation of coenzyme A (CoA) by fatty acids in the presence of added acyl-CoA synthetase. The acyl-CoA thus produced is oxidized by added acyl-CoA oxidase with generation of hydrogen peroxide that, in the presence of peroxidase, permits the oxidative condensation of 3-methy-N-ethyl-N(β-hydroxyethyl)-aniline with 4-aminoantipyrine to form a purple coloured adduct which can be measured colourimetrically at 550 nm. The method showed linearity over a NEFA concentration range of 0.002-2 mmol·L^{-1}. The lower limit of quantification (LLOQ) was 0.002 mmol·L^{-1} applying a sample volume of 10 μL plasma.

The binding of NiAc to plasma proteins in Sprague Dawley and obese Zucker rats was measured in Paper V by an automated equilibrium dialysis assay. After dialysis of plasma against a phosphate buffer at pH 7.0 over night, plasma and buffer samples were analyzed using LC-MS. The binding was measured at NiAc concentrations of and 1 and 10 μmol·L^{-1}. The fraction unbound, f_u, was calculated from the analyses in plasma and buffer.

3.5   Data analysis

The dose-response-time analysis (Paper I), was performed in WinNonlin 5.2 (Pharsight, CA, USA), whereas the pharmacokinetic and pharmacodynamic data in Papers II, IV and V, were modelled by means of nonlinear mixed-effects modelling using NONMEM (Version VI level 2.1, Icon Development Solutions, Elliot City, MD, USA).

3.6.1 Structural models

3.6.1.1 Dose-response-time analysis

Response *versus* time data, even in the absence of measured concentrations, inherently contain useful information about the turnover characteristics of a response (turnover rate, half-life of response), the drug's biophase kinetics (bioavailability, half-life) and the pharmacodynamic characteristics (potency, intrinsic activity) [96].

In the dose-response-time model developed in Paper I, the amount of drug in the biophase was used to drive the inhibitory drug mechanism function, and the elimination rate constant of the biophase and pharmacodynamic parameters were estimated in the regression analysis.

The biophase kinetics of NiAc was modelled as:

$$\frac{dA_b}{dt} = Input - k_e \cdot A_b \tag{1}$$

where A_b, *Input* and k_e are the drug amount in the biophase, the infusion regimen and the first-order elimination rate constant of NiAc from the biophase, respectively (Figure 4). The biophase kinetics of NiAc was then assumed to drive NEFA turnover via an inhibitory drug mechanism function:

$$I(A_b) = 1 - \frac{I_{max} \cdot A_b^{\gamma}}{ID_{50}^{\gamma} + A_b^{\gamma}} \tag{2}$$

where I_{max}, ID_{50} and γ are, respectively, the efficacy (maximum drug-induced inhibitory effect of formation of the NEFA response), the potency (amount in biophase reducing formation of response by 50 %) and the sigmoidicity factor, respectively. The mechanism of action of NiAc on NEFA plasma concentration R was modelled by means of inhibition of the turnover rate k_{in}:

$$\frac{dR}{dt} = k_{in} \cdot \frac{1}{M} \cdot I(A_b) - k_{out} \cdot R \tag{3}$$

where k_{in}, M, k_{out} and $I(A_b)$ are the turnover rate constant, the moderator, the fractional turnover rate constant and the inhibitory drug mechanism function (Equation 2), respectively (Figure 4). The moderator M then inhibits the production of R. The build-up and loss of M are governed by the first-order turnover rate constant k_{tol}:

$$\frac{dM}{dt} = k_{tol}(R - M) \tag{4}$$

The k_{tol} parameter will then govern the rate of tolerance development. The steady state response R_{SS} is expressed as:

$$R_{SS} = \sqrt{\frac{k_{in}}{k_{out}} \cdot I(A_b)} \tag{5}$$

where $I(A_b)$ can be translated to the inhibitory drug mechanism function for plasma concentration $I(C_p)$ using a volume of distribution allometrically scaled from guinea pigs (0.17 L, in-house data not shown).
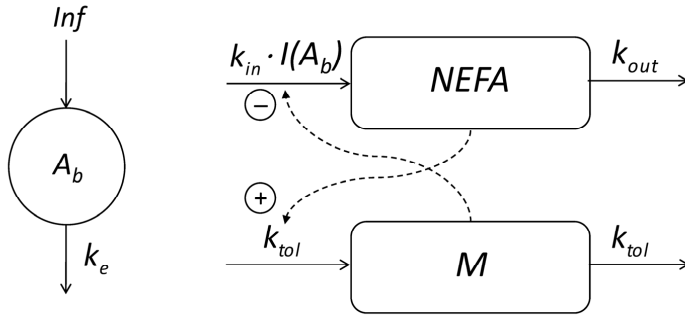
Figure 4. *Schematic illustration of the dose-response-time model of NEFA turnover in normal Sprague Dawley rats. The amount of NiAc in the biophase, governed by the infusion regimen (Inf) and the elimination rate (k_e), acts on the production of NEFA (R) via the inhibitory drug mechanism function $I(A_b)$. R acts linearly on the production of the moderator M, which in turn acts inversely on the production of R. The solid and dashed lines represent fluxes and control processes, respectively.*

3.6.1.2 Pharmacokinetics of NiAc in normal Sprague Dawley rats

The disappearance of NiAc from the gastrointestinal tract (Paper IV) was described as two parallel linear and nonlinear processes (Figure 5) given by:

$$\frac{dA_g}{dt} = -k_a \cdot A_g - \frac{V_{max,g} \cdot A_g}{K_{m,g} + A_g} \tag{6}$$

where A_g is the amount of drug in the gut, k_a is the first-order absorption rate constant, $V_{max,g}$ is the maximum absorption rate, and $K_{m,g}$ is the amount of drug in the gut when the absorption rate is 50 % of $V_{max,g}$. Including the bioavailability as a parameter in the modelling resulted in an estimate close to 1 and it was therefore fixed to 1 throughout the analysis.

The disposition of NiAc (Papers II and IV) was modelled as a two-compartment model with endogenous NiAc synthesis (*Synt*) and two parallel capacity-limited elimination processes (Figure 5) that probably correspond to glycine conjugation and amidation [130]. The exogenous input and disposition of NiAc were mathematically described by:

$$V_c \cdot \frac{dC_p}{dt} = Input + Synt - \frac{V_{max_1}}{K_{m_1} + C_p} \cdot C_p - \frac{V_{max_2}}{K_{m_2} + C_p} \cdot C_p - Cl_d \cdot C_p + Cl_d \cdot C_t \tag{7}$$

$$V_t \cdot \frac{dC_t}{dt} = Cl_d \cdot C_p - Cl_d \cdot C_t \tag{8}$$

where, respectively, C_p and C_t denote the NiAc concentration in the central (plasma) and peripheral compartments, V_c and V_t the central and peripheral volumes of distribution, *Input* the rate of intravenous infusion or oral administration of the drug, and *Synt* the endogenous synthesis rate of NiAc. The V_{max1} and K_{m1} parameters denote the maximal velocity and Michaelis-Menten constant of the high affinity elimination process, respectively, V_{max2} and K_{m2} the corresponding parameters for the low affinity elimination process, and Cl_d the intercompartmental distribution.

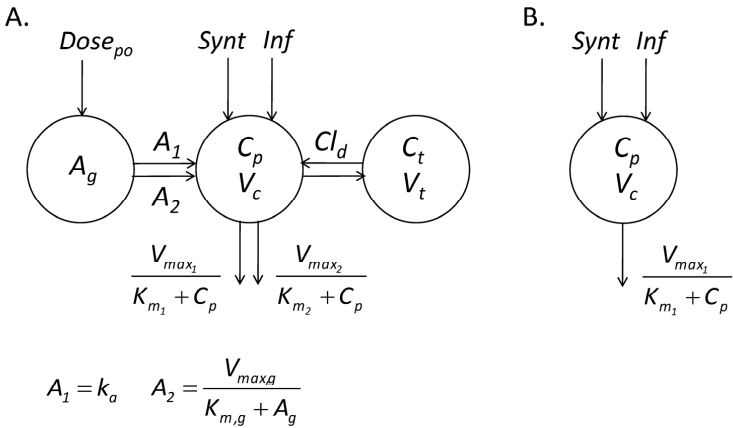$$A_1 = k_a \qquad A_2 = \frac{V_{max,g}}{K_{m,g} + A_g}$$

Figure 5. Schematic illustration of the absorption and disposition of NiAc in rats. (A) Normal Sprague Dawley rats (Papers II and IV). (B) Obese Zucker rats (Paper V). A_g denotes the amount of NiAc in the gut, and C_p and C_t the NiAc concentrations in plasma and the peripheral compartment, respectively. $Dose_{po}$ and Inf represent the oral dosing and intravenous infusions, respectively. A_1 and A_2 represent the linear and nonlinear absorption, respectively. The NiAc absorption and disposition parameters are k_a, $V_{max,g}$, $K_{m,g}$, V_c, V_t, V_{max1}, K_{m1}, V_{max2}, K_{m2}, Cl_d, and Synt (definitions in Table 5).

The total clearance Cl_{tot} can be expressed as:

$$Cl_{tot} = \frac{V_{max_1}}{K_{m_1} + C_p} + \frac{V_{max_2}}{K_{m_2} + C_p} \tag{9}$$

3.6.1.3 Pharmacokinetics of NiAc in obese Zucker rats
The disposition of NiAc in obese Zucker rats (Paper V) was modelled as a one-compartment model with endogenous synthesis (*Synt*) of NiAc and a single capacity-limited elimination (Figure 5). The model is mathematically described as:

$$V_c \cdot \frac{dC_p}{dt} = Input + Synt - \frac{V_{max_1}}{K_{m_1} + C_p} \cdot C_p \qquad (10)$$

where C_p denotes the NiAc concentration in the central compartment, V_c the central volume of distribution, *Input* the rate of intravenous infusion of NiAc, and *Synt* the endogenous synthesis rate. The V_{max1} and K_{m1} parameters are the maximal velocity and Michaelis-Menten constant, respectively.

3.6.1.4 Feedback model of NEFA in Sprague Dawley and obese Zucker rats

The hydrolysis of TG to NEFA and glycerol in adipocytes is inhibited by NiAc, with this inhibitory process $I(C_p)$ being described by:

$$I(C_p) = 1 - \frac{I_{max} \cdot C_p^\gamma}{IC_{50}^\gamma + C_p^\gamma} \qquad (11)$$

where C_p, I_{max}, IC_{50} and γ are, respectively, the NiAc plasma concentration, the maximum NiAc-induced inhibition of NEFA, the NiAc plasma concentration at 50 % reduction of the NEFA turnover rate (potency), and the sigmoidicity factor.

The feedback is governed by a moderator which is distributed over a series of 8 transit compartments, where moderator M_1 in the first compartment inhibits the adipocyte-dependent formation of R, and moderator M_8 in the eighth compartment stimulates the loss of R (Figure 6). The dual action of insulin on NEFA regulation is captured firstly by M_1, which denotes the rapid inhibition of the hydrolysis of TG to NEFA and glycerol in adipocytes [124, 125], and secondly by M_8, which represents the delayed stimulation of re-esterification of NEFA to TG [125, 126]. The moderator is affected by R via a first-order build-up of M ($k_{tol} \cdot R$). Each M compartment has a transit time of $1/k_{tol}$.

When NiAc inhibits the adipocyte-dependent formation of NEFA, NEFA will decrease, causing a reduction in the production of moderator and a subsequent decrease in M_1. As the formation of NEFA is inversely proportional to the moderator raised to the power of p (M_1^p), the formation of NEFA will increase when M_1 decreases. After a delay, the level of moderator M_8 in the final compartment will also fall, reducing the loss of NEFA. Eventually the concentrations of R and M_i (where i = 1, …, 8) will equilibrate.
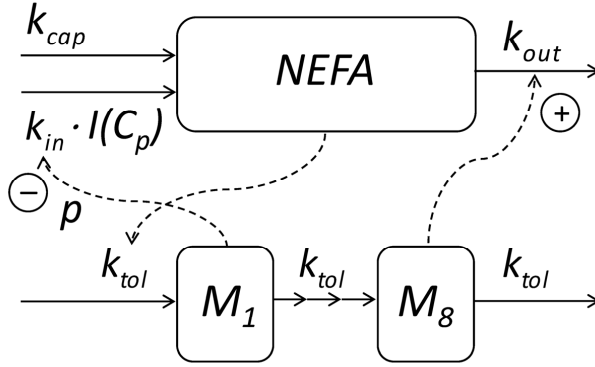
Figure 6. *Schematic illustration of the feedback model describing NiAc-induced changes in NEFA. NEFA and $M_{1,...,8}$ denote the response and moderator compartments, respectively. The NEFA turnover parameters are k_{in}, k_{out}, k_{tol}, k_{cap}, and p (definitions in Table 6). $I(C_p)$ is defined in Equation 11. The solid and dashed lines represent fluxes and control processes, respectively.*

A lower physiological limit of NEFA is observed at high NiAc concentrations probably due to lipoprotein lipase-catalyzed hydrolysis of TG to NEFA and glycerol in the capillaries. This NiAc-independent process is incorporated as a zero-order production term k_{cap} in the model:

$$\frac{dR}{dt} = k_{in} \cdot \frac{1}{M_1^p} \cdot I(C_p) + k_{cap} - k_{out} \cdot R \cdot M_8 \qquad (12)$$

where M_1 and M_8 are described above, and k_{in} is the turnover rate of NEFA, p the amplification factor, $I(C_p)$ the inhibitory drug mechanism function (Equation 11), k_{cap} the rate of formation of NEFA in capillaries, and k_{out} the fractional turnover rate of R. The turnover equations of the moderators are given by:

$$\frac{dM_1}{dt} = k_{tol} \cdot (R - M_1)$$
$$\frac{dM_2}{dt} = k_{tol} \cdot (M_1 - M_2)$$
$$\vdots$$
$$\frac{dM_8}{dt} = k_{tol} \cdot (M_7 - M_8)$$
$$\qquad (13)$$

where k_{tol} is the first order rate constant of moderator turnover.

The turnover rate k_{in} of NEFA is derived and expressed as:

$$k_{in} = (k_{out} \cdot R_0^2 - k_{cap}) \cdot R_0^p \tag{14}$$

where R_0 is the baseline NEFA concentration and p the amplification factor. The extent of tolerance can be approximated by comparison of the full feedback system (Equations 12 and 13) and a non-tolerant turnover system. In the non-tolerant system all moderators remain at baseline at all times ($M_i(t) = M_0 = R_0$) and Equations 12 and 13 can then be simplified to:

$$\frac{dR}{dt} = k_{in} \cdot \frac{1}{R_0^p} \cdot I(C_p) + k_{cap} - k_{out} \cdot R \cdot R_0 \tag{15}$$

3.6.1.5 Initial parameter estimates and steady state expressions
The turnover rate k_{in} of NEFA was estimated in the modelling process as a function of R_0, k_{out} and k_{cap} according to Equation 14.

The baseline concentration R_0 was obtained from the predose level of NEFA. Following a high dose of NiAc ($C_p \gg IC_{50}$), Equation 12 can be approximated by:

$$\frac{dR}{dt} \approx k_{cap} - k_{out} \cdot R \cdot M_8 \tag{16}$$

Provided k_{cap} is initially much less than $k_{out} \cdot R \cdot R_0$, Equation 16 can be simplified to:

$$\frac{dR}{dt} \approx -k_{out} \cdot R \cdot R_0 \tag{17}$$

where M_8 is approximated by R_0. Thus, the initial downswing of R on a semi-logarithmic plot gives a slope of $-k_{out} \cdot R_0$. The k_{out} parameter can then be estimated from the ratio of the slope to R_0.

The lower physiological limit of NEFA was reached following the highest dose of NiAc. Assuming complete inhibition (*i.e.*, $I(C_p) = 0$) and that both R and M_8 are equal to R_{min}, k_{cap} can be estimated from:

$$k_{cap} \approx k_{out} \cdot R_{min}^2 \tag{18}$$

where R_{min} denotes the minimum response following a 30 min infusion.

The rebound is governed by k_{tol} and it takes 3-4 $t_{1/2,ktol}$ for the response to re-stabilize at baseline after rebound. The length of rebound following a 30 min infusion of NiAc is approximately 40 min and $t_{1/2,ktol}$ is subsequently around 10 min. An initial estimate of k_{tol} can then be roughly approximated according to:

$$t_{1/2,ktol} = \frac{ln(2)}{(p+1)k_{tol}} \tag{19}$$

The IC_{50} was approximated as the concentration of NiAc resulting in a half maximal response following a 30 min infusion. The sigmoidicity (γ) and amplification (p) factors were initially both set equal to unity.

The steady state values for the response R and the moderators M_i ($i = 1,…, N$) of the feedback model, formulated in Equations 12 and 13, are given by:

$$R = M_1 = \cdots = M_N = R_{ss} \tag{20}$$

where the steady state concentration R_{ss} is the unique solution of the equation:

$$\frac{dR}{dt} = \frac{k_{in}}{R_{ss}^p} \cdot I(C_p) + k_{cap} - k_{out} \cdot R_{ss}^2 = 0 \tag{21}$$

in which

$$k_{in} = (k_{out} \cdot R_0^2 - k_{cap}) \cdot R_0^p \tag{22}$$

and R_0 is the baseline response. In general it is not possible to write the solution R_{ss} of Equation 21 as an explicit expression when k_{cap} is nonzero.

For the obese animals, k_{cap} could not be estimated and was therefore fixed to zero throughout the analysis. Equation 21 can then be simplified and solved for R_{ss}:

$$R_{SS,obese} = \left(\frac{k_{in}}{k_{out}} \cdot I(C_p) \right)^{1/(2+p)} \tag{23}$$

3.6.2 Statistical models

Pharmacokinetic and pharmacodynamic software (*e.g.* WinNonlin and NONMEM) iteratively search for the parameter estimates of a predefined model, resulting in the best graphical description of experimental data. In

traditional pharmacokinetic and pharmacodynamic analysis, a two-stage approach is often applied, with a model being fitted to each individual separately, and the inter-individual variability in the parameters being calculated subsequently [131, 132]. This method requires frequent sampling from each individual, and to sufficiently describe the experimental data in each individual, different structural models might be applied, biasing calculations of inter-individual variability. A two-stage approach can also lead to overestimation of the inter-individual variability as this method does not discriminate between random residual variability (unexplained variability) and variability in the parameters. An alternative approach is to use nonlinear mixed-effects modelling, where a minimum of two levels of variability (referred to as random effect parameters) are identified and separated, in addition to the parameters of the structural model (referred to as fixed effects parameters). The first level of variability handles random residual variability, which corresponds to the unexplained variability such as model misspecification and experimental errors. The second level explains variability of parameters between subjects and occasions. In nonlinear mixed-effects modelling, the structural and statistical models are fitted to the observations simultaneously, allowing discrepancies in data density and parameter estimates between individuals. A disadvantage of this method is that it can be computer intensive and time consuming.

3.6.2.1 Statistical models and numerics applied in Papers II, IV and V

All fixed effects parameters were assumed to be log-normally distributed and the inter-individual variability was, accordingly, modelled as exponential models for all parameters. The random residual variability in the pharmaco-kinetic analysis of NiAc was modelled as a function of proportional and additive error in Paper II, whereas a single proportional error model was used in Papers IV and V. In the feedback modelling of NEFA in Papers II and V, a proportional error model was used, whereas an additive model was used in Paper IV.

The Laplacian estimation method with interactions was used in the pharmacokinetic analysis of NiAc in Paper IV, and without interactions in Papers II and V. The turnover of NEFA was analyzed by the Laplacian estimation method without interactions.

The individual pharmacokinetic parameters of NiAc were introduced as fixed parameters in the analysis of NEFA data.

4   Results and discussion

4.1   Dose-response-time analysis (Paper I)

The rationale behind modelling dose-response-time data is that response-time relationships contain information about the underlying kinetics of a drug in the biophase. By using appropriate modelling, it should be possible to derive this kinetic information from the pharmacodynamic data. To achieve this, a virtual compartment that represents the biophase in which the drug amount is driving the pharmacodynamics is usually included in the model. Early descriptions of this concept were given by Levy [133-135] and Smolen [136], and further developed by Verotta and Sheiner [137]. Dose-response-time models have been applied to data in the fields of anaesthesia-logy [138, 139], lipolysis [140], antinociception, cortisol secretion and body temperature regulation [96].

Using a multiple intravenous infusion technique, NiAc was shown to reduce plasma NEFA concentrations in rats by 67-86 % below baseline, followed by a post-infusion rebound of 28-150 % above predose baseline (Figure 7).

The dose-response-time feedback model described in Section 3.6.1.1 was fitted to individual response-time data from the different studies (see Table 1). The average final parameter estimates and their precision (CV %) are shown for Study 1 in Table 4, together with the range of each estimate from applying the model to all 4 studies. The model-predicted NEFA concentrations were consistent with the experimental data (Figure 7) and the precision of the estimates was high for all parameters (Table 4). The final parameter estimates from Study 1 fell on either the lower or upper boundary of the range for most parameters. However, the challenging design of the multiple consecutive infusions regimen in Study 1 may have revealed more correct behaviour of the system than the parameter ranges as the latter also included Studies 2-4, each with one animal.
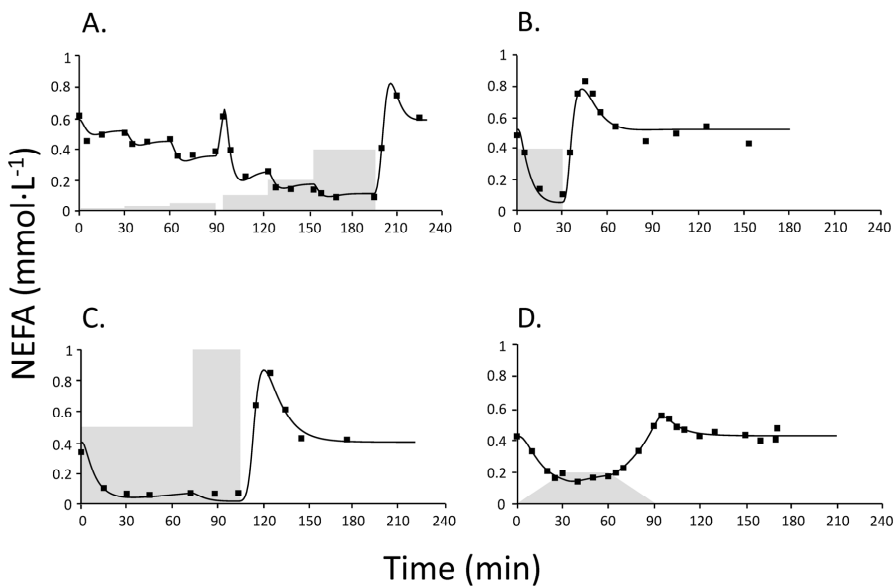
Figure 7. *Individual time-courses of the plasma NEFA concentration ($mmol \cdot L^{-1}$) following constant rate intravenous infusion of NiAc to normal Sprague Dawley rats. NiAc administration commenced at time t = 0 min. Symbols represent observed concentrations for a single animal and solid black lines the model-predicted response. The grey areas symbolize the duration for which different doses were infused. (A) Study 1 – Consecutive infusions of 0.8, 1.6, 3.2, 6.4, 12.8 and 25.6 $nmol \cdot min^{-1}$, with the infusion rate doubled every 30 min and infusion stopped at 196 min. The break at 90-96 min was due to changing the syringe. (B) Study 2 – Infusion of 25.6 $nmol \cdot min^{-1}$ for 30 min. (C) Study 3 – Consecutive infusions of 32 and 64 $nmol \cdot min^{-1}$, with the infusion rate increased at 73 min and infusion stopped at 104 min. (D) Study 4 – Infusion rate increased stepwise every 3 min for 30 min from 0 to 13 $nmol \cdot min^{-1}$, held constant at 13 $nmol \cdot min^{-1}$ for 30 min, and decreased stepwise every 3 min for 30 min from 13 to 0 $nmol \cdot min^{-1}$.*

By dividing the ID_{50} value by the volume of distribution (0.17 L) scaled allometrically from guinea pig, IC_{50} was estimated to be 0.038 $\mu mol \cdot L^{-1}$.

The NEFA datasets analyzed in Paper I were originally designed to assess qualitatively the behaviour of plasma NEFA concentrations after different NiAc provocations. As a result, the sampling schedule was intended to detect the maximum and minimum response to NiAc, and to demonstrate the rebound phenomenon. Hence, the data collected were exploratory rather than optimal for parameter estimation. However, although the biophase kinetic model may not have precisely represented the plasma kinetics of NiAc, it still contributed to the estimation of the system (*e.g.* k_{out}, k_{tol}) and drug parameters (ID_{50}, γ).

Table 4. *Final parameter estimates from the dose-response-time analysis in Study 1 (Paper I)*

Parameter	Estimate ± CV %[*] (Range)[**]
R_0 (mmol·L^{-1})	0.55 ± 3.6 (0.41-0.55)
k_{out} (min^{-1})	0.30 ± 31 (0.14-0.35)
k_{tol} (min^{-1})	0.079 ± 27 (0.023-0.079)
ID_{50} (µmol)	0.0065 ± 31 (0.0065-0.058)
γ	1.4 ± 9.2 (1.4-3.7)
k_e (min^{-1})	0.44 ± 18 (0.21-0.44)

[*] *Final estimates from Study 1 presented as mean ± CV % (n=10); CV % is the precision of the parameter estimate, calculated as (SE/estimate)·100 in WinNonlin*

[**] *Range from all 4 studies in Paper 1 (n=1 for each of Studies 2-4)*

Smolen [136] assumed that dose-response-time analysis might be expected to fail unless linear kinetics, linear dynamics, time-constant parameters, no active metabolites, and no tolerance or rebound pertained. However, it has been demonstrated that, with appropriate design, the drug effect can be modelled successfully in spite of indirect action [96, 140], active metabolites [140], and feedback/time dependencies [96].

This analysis exemplifies the possibility of assigning kinetic forcing functions in pharmacodynamic modelling for the purpose of characterizing a drug's response (*i.e.* discriminating between system- and drug-specific parameters, and optimizing the design of subsequent studies). However, crucial determinants of the success of modelling dose-response-time data are dose selection, multiple dosing, and an optimized sampling regimen [96, 140].

4.2 Pharmacokinetics of NiAc

4.2.1 Normal Sprague Dawley rats (Papers II and IV)

Observed plasma concentrations of NiAc following infusions and oral administration of NiAc are shown in Figure 8. The highest NiAc concentration (223 µmol·L^{-1}) was observed after oral administration of 812 µmol·kg^{-1} NiAc (Figure 8D). The nonlinear disposition of NiAc became pronounced at high drug concentrations. The NiAc concentration-time profiles displayed a plateau after oral dosing, which could indicate nonlinear absorption.
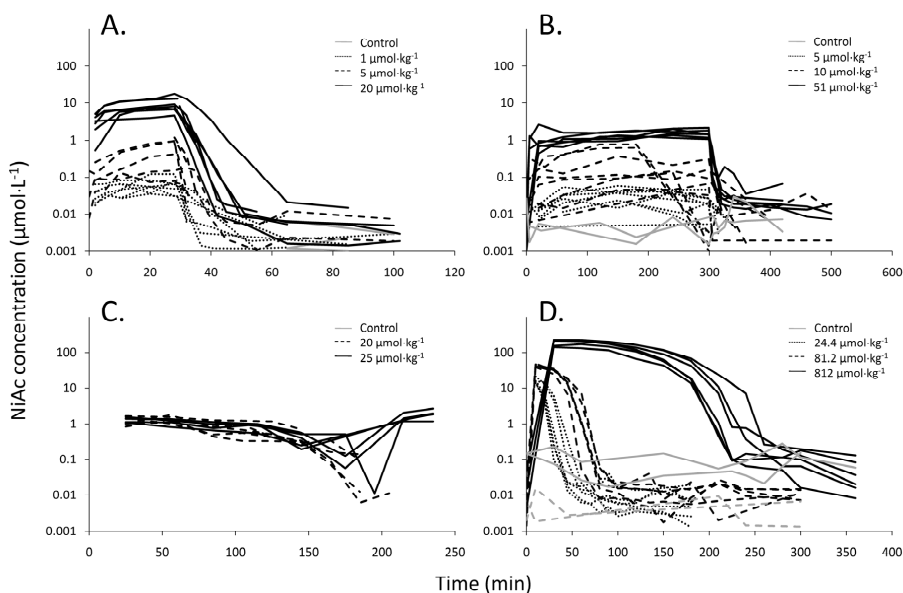
Figure 8. *Observed plasma NiAc concentration-time profiles in normal Sprague Dawley rats during and after vehicle or NiAc administration. Control groups received vehicle according to the same regimen as their respective NiAc-treated group. (A) 30 min infusion of 0, 1, 5 or 20 μmol NiAc per kg of body weight; (B) 300 min infusion of 0, 5, 10 or 51 μmol·kg^{-1}; (C) 30 min infusion of 0 or 5 μmol·kg^{-1}, followed by a stepwise decrease in infusion rate every 10 min over 180 min (total dose of 20 μmol·kg^{-1}, dashed) and a subsequent 30 min infusion of 0 or 5 μmol·kg^{-1} commencing at 210 min (total dose of 25 μmol·kg^{-1}, solid); (D) oral dose of 0, 24.4, 81.2 or 812 μmol·kg^{-1}. The NiAc concentrations in the two control animals in (C) fell below the LLOQ. In (B), no samples were taken between 200 and 300 min in two rats given 10 μmol·kg^{-1}.*

The reason for modelling NiAc concentration-time data was to obtain an individual time curve for each animal that could be used to drive the NEFA concentration time-course. A two-compartment model with endogenous NiAc synthesis and two parallel capacity-limited elimination pathways, probably corresponding to glycine conjugation and amidation, described the disposition of NiAc consistently (Figure 9). Iwaki *et al.* [130] showed that the glycine conjugation forming nicotinuric acid was capacity-limited in rats *in vivo*, and also provided weak evidence that the amidation pathway was capacity-limited. The absorption from the gastrointestinal tract was described in the current studies by a parallel nonlinear and linear process (Equation 6).
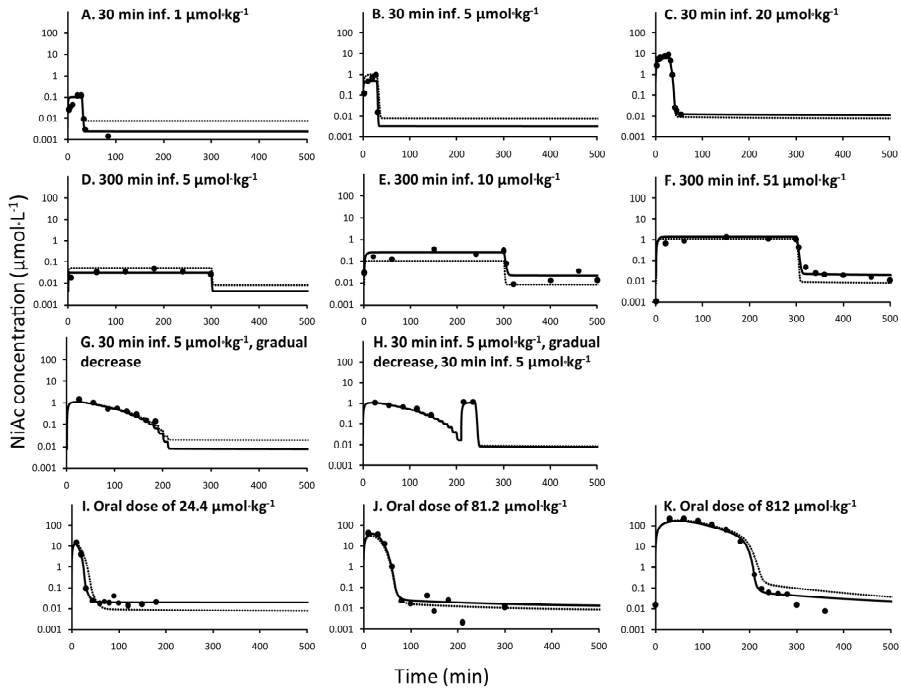
Figure 9. *Representative model fits of NiAc plasma concentration-time data in normal Sprague Dawley rats after infusion (A-H) and oral dosing (I-K) of NiAc. Solid and dotted lines represent individual and population fits, respectively. Infusion of (A) 1 μmol·kg^{-1}, (B) 5 μmol·kg^{-1}, and (C) 20 μmol·kg^{-1} over 30 min; (D) 5 μmol·kg^{-1}, (E) 10 μmol·kg^{-1}, and (F) 51 μmol·kg^{-1} over 300 min; (G) total dose of 20 μmol·kg^{-1} administered as 5 μmol·kg^{-1} over 30 min, followed by a stepwise decrease in infusion rate every 10 min for 180 min; (H) total dose of 25 μmol·kg^{-1} administered as 5 μmol·kg^{-1} over 30 min, followed by a stepwise decrease in infusion rate every 10 min for 180 min, and another 5 μmol·kg^{-1} infusion over 30 min. Oral dose of 24.4 (I), 81.2 (J) or 812 (K) μmol·kg^{-1}.*

The NiAc parameter estimates in normal Sprague Dawley rats obtained in Papers II and IV are shown in Table 5. In Paper II, the additive error is small, but only a proportional error model resulted in increased objection function value (OFV) and impaired curve-fit. In Paper IV, the intercompartmental distribution Cl_d was estimated to 0.00085 L·min^{-1}·kg^{-1} which corresponds to a blood flow in humans around 20 mL·min^{-1}. The peripheral compartment would then represent a tissue that is only perfused to a tenth of that of adipose tissue. This indicates that a one-compartment model might suffice to describe the disposition of NiAc.

Table 5. *Typical NiAc pharmacokinetic parameter estimates and inter-individual variability (IIV), with corresponding relative standard errors (RSE %) for normal Sprague Dawley (Papers II and IV) and obese Zucker (Paper V) rats*

Parameter	Sprague Dawley rats (Paper II)		Sprague Dawley rats (Paper IV)		Obese Zucker rats (Paper V)	
	Estimate (RSE %)	IIV (RSE %)	Estimate (RSE %)	IIV (RSE %)	Estimate (RSE %)	IIV (RSE %)
V_{max1} (μmol·min^{-1}·kg^{-1})	0.0573 (1.57)	-	0.0871 (22.8)	92.7 (27.5)	1.59 (13.9)	21.4 (234)
K_{m1} (μmol·L^{-1})	0.00468 (1.97)	-	0.235 (29.2)	-	18.9 (21.5)	-
V_{max2} (μmol·min^{-1}·kg^{-1})	1.46 (4.20)	98.2 (24.8)	7.09 (39.6)	29.1 (43.6)	-	-
K_{m2} (μmol·L^{-1})	16.6 (6.20)	-	74.5 (43.4)	-	-	-
V_c (L·kg^{-1})	0.345 (0.559)	-	0.393 (5.29)	-	0.323 (12.4)	-
V_t (L·kg^{-1})	3.54 (7.66)	-	0.172 (35.2)	-	-	-
Cl_d (L·min^{-1}·kg^{-1})	0.0203 (3.08)	54.5 (88.6)	0.000852 (27.8)	-	-	-
$Synt$ (μmol·min^{-1}·kg^{-1})	0.0346 (4.10)	15.8 (62.5)	0.00355 (23.3)	109 (34.7)	0.00280 (10.1)	95.3 (115)
k_a (min^{-1})	-	-	0.00477 (33.5)	-	-	-
$V_{max,g}$ (μmol·min^{-1}·kg^{-1})	-	-	2.96 (21.3)	10.8 (93.1)	-	-
$K_{m,g}$ (μmol·kg^{-1})	-	-	20.5 (29.6)	-	-	-
σ_1 (%)	32.4 (18.6)	-	42.8 (5.16)	-	40.0 (26.3)	-
σ_2 (μmol·L^{-1})	0.0000647 (5.80)	-	-	-	-	-

V_{max1} = maximal velocity, high affinity pathway 1, K_{m1} = Michaelis Menten constant, high affinity pathway 1, V_{max2} = maximal velocity, low affinity pathway 2, K_{m2} = Michaelis Menten constant, low affinity pathway 2, V_c = central volume of distribution, V_t = peripheral volume of distribution, Cl_d = intercompartmental distribution, $Synt$ = endogenous NiAc synthesis rate, k_a = first order absorption rate constant, $V_{max,g}$ = maximal absorption rate, $K_{m,g}$ = amount of drug in gut at half maximal absorption rate, σ_1 = residual proportional error, σ_2 = residual additive error

In Figure 10, total clearance Cl_{tot}, calculated using parameter estimates in each of Papers II and IV, is plotted against NiAc concentration, together with total clearance from Iwaki *et al.* [130]. At low NiAc concentrations total clearances differed considerably in these studies, whereas at concentrations above ∼ 0.5 μmol·L^{-1} the differences decreased. This may be due to the different NiAc concentration ranges in the three studies (0.001-20 μmol·L^{-1} in Paper II, 0.001-220 μmol·L^{-1} in Paper IV, and 0.8-800 μmol·L^{-1} in Iwaki *et al.)* As the LLOQ in Iwaki *et al.* was 0.8 μmol·L^{-1}, there is high uncertainty in the calculated total clearance at concentrations below their LLOQ. The rat strains also differed between these studies, with Papers II and IV using Sprague Dawley rats, and Iwaki *et al.* Wistar. Finally, Iwaki *et al.* did not include an endogenous synthesis parameter or a mixed-effects modelling approach.
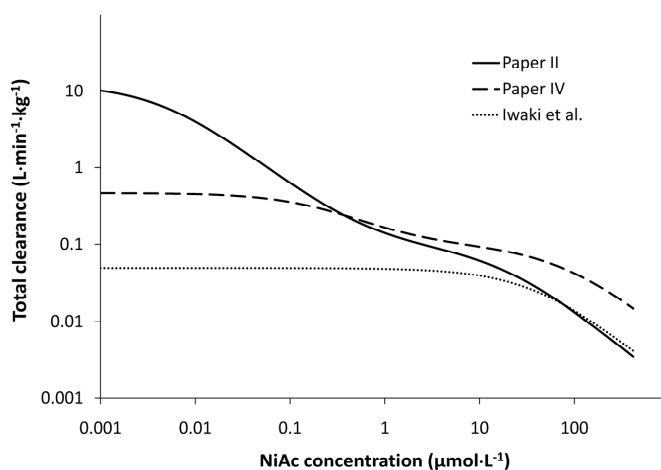

Figure 10. Total clearance versus NiAc concentration in normal Sprague Dawley rats, calculated from the NiAc disposition parameters in Papers II and IV (Table 5), and in Iwaki et al. [130]. The LLOQ was 0.001 μmol·L^{-1} in Papers II and IV and 0.8 μmol·L^{-1} in Iwaki et al. The curves for Papers II and IV were derived using Equation 9 in Section 3.6.1.2 and the final parameter estimates in Table 5. For Iwaki et al., a single capacity-limited elimination model was used, with V_{max1} and K_{m1} of 1.9 μmol·min^{-1}·kg^{-1} and 39 μmol·L^{-1}, respectively.

In terms of the discrepancies between Papers II and IV, differences in methodology that may have influenced the results include the amounts of available data, the provocations included in the analysis, the range of NiAc exposure, the routes of NiAc administration, over-parameterisation, and changes in the differential equation solver and the method of estimation. However, it is important to note that the primary purpose of the NiAc model was to drive the pharmacodynamics and an acceptable description of the

observed individual concentration time-courses was therefore the primary goal of the pharmacokinetic analysis.

The free fraction of NiAc in plasma (f_u) in Sprague Dawley rats was 81 and 74 %, at 1 and 10 µmol L^{-1} NiAc, respectively, resulting in an average of 78 %. This is discussed together with the obese rats in Section 4.2.2.

4.2.2 Obese Zucker rats (Paper V)

Observed NiAc concentration time-courses for obese Zucker rats are plotted in Figure 11, with comparable data from normal Sprague Dawley rats. NiAc infusion rates of 0.67 µmol·min^{-1}·kg^{-1} (20 µmol·kg^{-1} over 30 min, Figure 11A) and 0.17 µmol·min^{-1}·kg^{-1} (51 µmol·kg^{-1} over 300 min, Figure 11B) resulted in slightly higher plasma concentrations in the obese rats compared to the normal rats. The highest observed NiAc concentrations were 23.3 and 17.9 µmol·L^{-1} in the obese and normal rats, respectively.

Compared to normal rats, the disposition of NiAc was altered in obese rats, being adequately described (Figure 11C, D) by a one-compartment model with endogenous NiAc synthesis and a single capacity-limited elimination process. Not only has it been reported that the pharmacokinetics of drugs may be altered in disease [141-143], but it has been proposed that obesity influences the distribution and clearance of compounds [119-123]. The altered disposition of NiAc in obese rats compared to normal rats was, therefore, not surprising.

The disposition parameters of NiAc in obese rats are summarized in Table 5. The structural parameters were estimated with high precision, but the inter-individual variability (IIV) was estimated with low certainty in this preliminary analysis. However, as the aim of modelling NiAc concentration-time data was to find individual time profiles that could drive the individual NEFA concentration time-courses, the present analysis fulfilled this aim. Nevertheless, further modelling is required to estimate the inter-individual variability with higher certainty and to enable definite conclusions about NiAc disposition in normal and obese rats to be drawn.

The free fraction f_u of NiAc in obese Zucker rats at 1 and 10 µmol·L^{-1} NiAc was, respectively, 94 and 102 %, with an average of 98 %. Plasma protein binding was slightly lower in the obese rats than in normal rats (average f_u 78 %), which is consistent with the possible competition of NEFA for binding to plasma proteins [144]. Because NiAc is rapidly eliminated and perfusion of the liver is the rate-limiting step, the unbound NiAc concentration is

dependent on f_u [145], suggesting that a difference in protein binding between normal and obese rats might be important. However, as the molar concentration of plasma albumin is around 600 µmol·L^{-1} and the highest observed NiAc concentration in obese rats was only around 20 µmol·L^{-1}, the impact of protein binding would be negligible and unlikely to account for other differences in the NiAc-NEFA system of the two strains of rats.
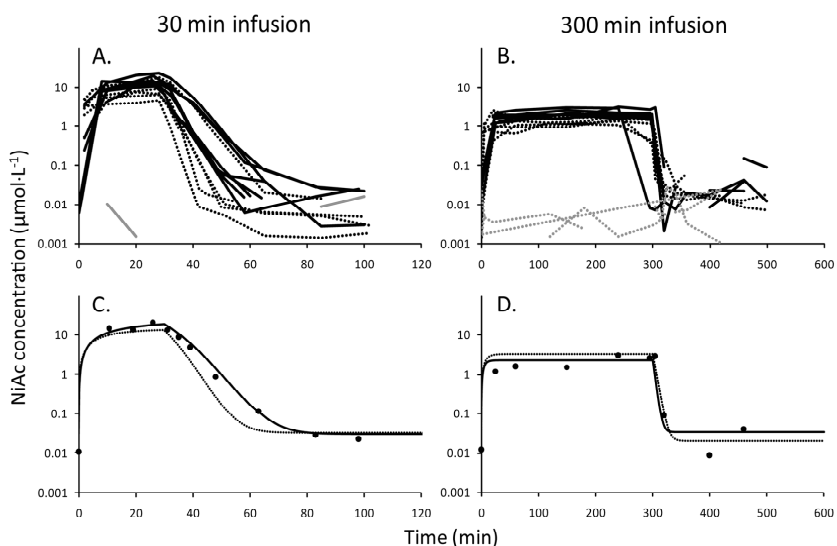

Figure 11. *Plasma NiAc concentration-time profiles during and after infusion of vehicle (grey) or NiAc (black). Observed data for normal (dotted lines) and obese (solid lines) rats (A and B), and predicted data for obese rats (C and D). Control groups received vehicle according to the same regimen as their respective NiAc-treated group. (A) 30 min of 0 or 20 µmol NiAc per kg of body weight; (B) 300 min of 0 or 51 µmol·kg^{-1}. The NiAc baseline concentration could only be quantified in the limited number of control samples which were at or above the LLOQ (≥ 0.001 µmol·L^{-1}). Individual (solid line) and population (dotted line) predicted NiAc plasma concentration time-course in a representative obese rat after 30 min of 20 µmol·kg^{-1} (C), and 300 min of 51 µmol·kg^{-1} (D) NiAc.*

4.3 Feedback modelling of NEFA

4.3.1 Normal Sprague Dawley rats (Papers II and IV)

Observed individual NEFA concentration-time profiles obtained after NiAc administration are shown for normal rats in Figure 12. Baseline NEFA concentrations ranged from 0.29 to 1.2 µmol·L^{-1}. NiAc administration rapidly decreased the concentration to approximately 10 % of the predose baseline level. Increased NiAc exposure did not further reduce NEFA concentrations,

suggesting a lower physiological limit of NEFA of around 0.05 mmol·L^{-1} (LLOQ = 0.002 mmol·L^{-1}). Following abrupt decreases in NiAc exposure, NEFA concentration increased rapidly, with marked rebound (to between 118 and 362 % of the predose baseline level) after all dose regimens. The rebound amplitude depended on both the extent and duration of NiAc exposure, being increased after high and prolonged exposure. Post-rebound oscillatory behaviour was most noticeable following long (300 min) infusions (Figure 12B).
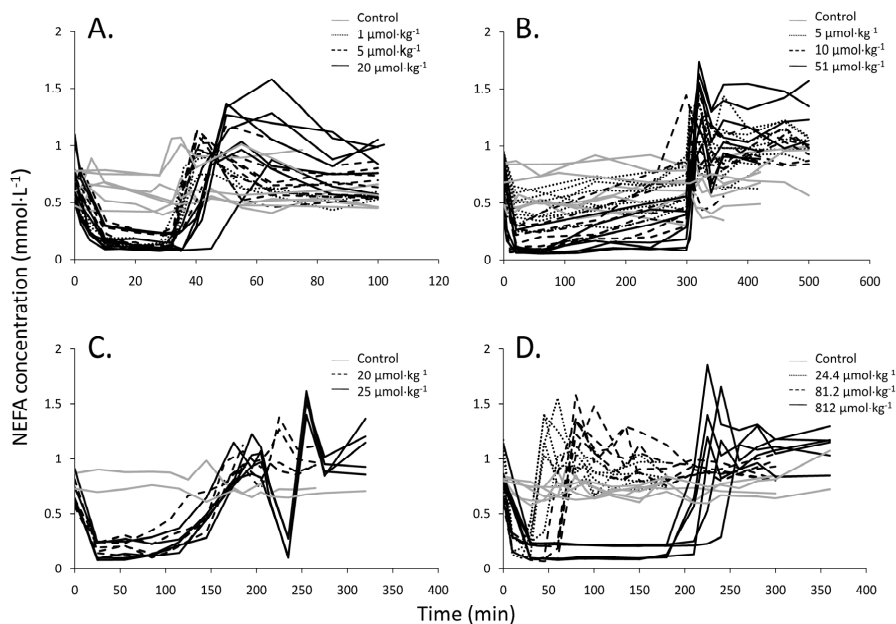

Figure 12. *Observed plasma NEFA concentration-time profiles in normal Sprague Dawley rats during and after vehicle or NiAc administration. Control groups received vehicle according to the same regimen as their respective NiAc-treated group. (A) 30 min infusion of 0, 1, 5 or 20 μmol NiAc per kg of body weight; (B) 300 min infusion of 0, 5, 10 or 51 μmol·kg^{-1}; (C) 30 min infusion of 0 or 5 μmol·kg^{-1}, followed by a stepwise decrease in infusion rate every 10 min over 180 min (total dose of 20 μmol·kg^{-1}, dashed) and a subsequent 30 min infusion of 0 or 5 μmol·kg^{-1} commencing at 210 min (total dose of 25 μmol·kg^{-1}, solid); (D) oral dose of 0, 24.4, 81.2 or 812 μmol·kg^{-1}. NEFA concentrations were stable in individual control animals, but there was large variability between animals.*

The NiAc-NEFA system showed adaptation, a lower physiological limit, rebound and post-rebound oscillatory behaviour. Representative individual and population predictions superimposed on experimental data after different dose regimens and routes of administration are shown in Figure 13.
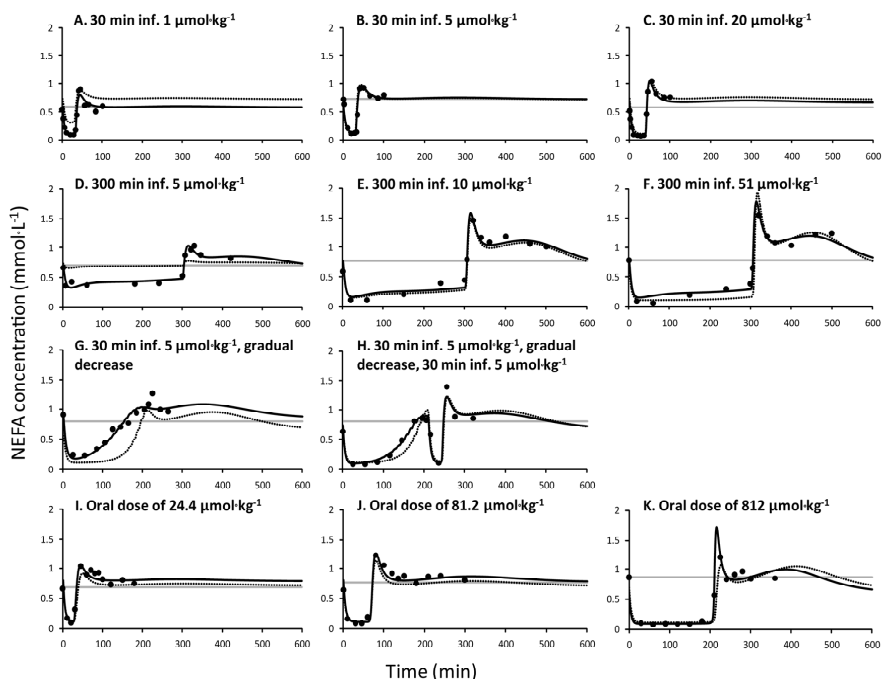

Figure 13. *Representative model fits of NEFA plasma concentration-time data in normal Sprague Dawley rats after infusion (A-H) and oral administration (I-K) of NiAc. Solid and dotted lines represent individual and population fits, respectively, and grey lines the individually predicted baseline. Infusion of (A) 1 μmol·kg⁻¹, (B) 5 μmol·kg⁻¹, and (C) 20 μmol·kg⁻¹ over 30 min; (D) 5 μmol·kg⁻¹, (E) 10 μmol·kg⁻¹, and (F) 51 μmol·kg⁻¹ over 300 min; (G) total dose of 20 μmol·kg⁻¹ administered as 5 μmol·kg⁻¹ over 30 min, followed by a stepwise decrease in infusion rate every 10 min for 180 min; (H) total dose of 25 μmol·kg⁻¹ administered as 5 μmol·kg⁻¹ over 30 min, followed by a stepwise decrease in infusion rate every 10 min for 180 min, and another 5 μmol·kg⁻¹ infusion over 30 min. Oral dose of 24.4 (I), 81.2 (J), and 812 (K) μmol·kg⁻¹.*

Insulin, one of several NEFA regulators, primarily affects NEFA homeostasis by rapidly inhibiting hydrolysis of TG to NEFA and glycerol [124, 125], and by stimulating re-esterification of NEFA to TG through a more slowly acting path [125, 126]. The feedback model used here was built on mechanistic principles, mimicking insulin's regulatory impact on NEFA homeostasis by introducing a moderator which acted via a series of transit compartments; with moderator in the first and last compartments representing the rapid and slow mechanisms, respectively. The model successfully mimicked the observed non-intuitive changes in NEFA concentration after different

patterns of NiAc exposure produced by different rates and routes of NiAc administration.

The typical parameters in normal Sprague Dawley rats were estimated with high precision (Table 6). The system parameter estimates (k_{in}, k_{out}, k_{tol}, k_{cap} and p) were generally in good agreement between the two studies, with the exception that, compared to Paper II, k_{out} was reduced by 34 % in Paper IV and k_{in} (estimated as a secondary parameter) was increased by 36 %. The drug parameters γ and IC_{50} were increased by 47 and 52 %, respectively, in Paper IV compared to Paper II. These discrepancies may reflect differences in experimental design and/or analytical methods, as outlined in Section 4.2.1.

The contribution of the baseline NiAc concentration to the reduction in NEFA is probably negligible because NiAc potency (*i.e.* NEFA IC_{50}, Table 6) was 0.045 and 0.068 µmol·L^{-1}, and the endogenous NiAc concentration 0.007 and 0.008 µmol·L^{-1} in Papers II and IV, respectively.

The lower limit of plasma NEFA concentrations was captured by means of a separate parameter k_{cap}, mimicking the non-adipocyte dependent release of NEFA into plasma. Because a lower physiological limit is also seen following administration of other GPR109A agonists (*e.g.* acipimox [146]), it is suggestive of a system- rather than drug-specific parameter. Consequently, substituting k_{cap} for I_{max} in order to capture the lower physiological limit would not be mechanistically correct. Simultaneous estimation of k_{cap} and I_{max} would be difficult since both parameters are determined from the minimum response and will therefore be highly correlated unless data of both full and partial agonists are evaluated simultaneously.

Ideally, the number of transit compartments should be estimated as a parameter in the model, as this makes it possible to add inter-individual variability of the number of compartments, as shown by Sun and Jusko [147] and Savic *et al*. [148]. However, these methods could not be applied, because they were based on the assumption that there was no continuous input to the first transit compartment, whilst here, all eight compartments were filled. Thus, the optimal number of compartments N was estimated to be 8 by manually increasing N until the best fit and minimum OFV was established. By increasing N, the oscillatory behaviour of the response became more pronounced. For $N < 6$, oscillatory rebound was not adequately captured and OFV was increased.

Table 6. *Typical pharmacodynamic (NEFA response) parameter estimates and inter-individual variability (IIV) with corresponding relative standard errors (RSE %) for normal Sprague Dawley (Papers II and IV) and obese Zucker (Paper V) rats*

Parameter	Sprague Dawley rats (Paper II)		Sprague Dawley rats (Paper IV)		Obese Zucker rats (Paper V)	
	Estimate (RSE %)	IIV (RSE %)	Estimate (RSE %)	IIV (RSE %)	Estimate (RSE %)	IIV (RSE %)
R_0 (mmol·L^{-1})	0.606 (3.51)	29.0 (43.1)	0.736 (4.33)	21.6 (27.3)	1.06 (6.52)	14.8 (34.6)
k_{out} (L·mmol^{-1}·min^{-1})	0.411 (9.22)	48.2 (35.6)	0.273 (10.2)	42.7 (11.3)	0.0986 (24.5)	69.5 (62.9)
k_{tol} (min^{-1})	0.0267 (3.40)	-	0.0231 (1.90)	-	0.0297 (10.2)	-
k_{cap} (mmol·L^{-1}·min^{-1})	0.0318 (6.51)	-	0.0230 (10.1)	-	0 (fixed)	-
k_{in} (mmol^2·L^{-2}·min^{-1})*	0.0650	-	0.0884	-	0.125	-
p	1.21 (6.64)	-	1.13 (2.76)	-	2.01 (15.8)	-
IC_{50} (µmol·L^{-1})	0.0446 (7.20)	101 (46.1)	0.0680 (15.4)	131 (34.9)	0.0538 (56.5)	135 (43.4)
γ	1.48 (3.79)	-	2.18 (4.48)	-	0.347 (9.34)	-
I_{max}	1 (fixed)	-	1 (fixed)	-	1 (fixed)	-
σ_1 (%)	22.1 (8.51)	-	-	-	12.0 (19.9)	-
σ_2 (mmol·L^{-1})	-	-	0.00913 (2.63)	-	-	-

R_0 = baseline NEFA concentration, k_{out} = fractional turnover rate constant, k_{tol} = turnover rate constant of moderator, k_{cap} = NEFA formation in the capillaries, k_{in} = turnover rate constant of NEFA, p = amplification factor, IC_{50} = potency, γ = sigmoidicity factor, I_{max} = efficacy, σ_1 = residual proportional error, σ_2 = residual additive error. * calculated as secondary parameter

4.3.2 Obese Zucker rats (Paper V)

Observed individual NEFA concentration-time profiles after NiAc administration to obese (Paper V) and normal (Papers II and IV) rats are shown in Figure 14. The differences are summarized qualitatively in Table 7. In normal rats, plasma NEFA concentrations decreased rapidly to a lower physiological limit of 0.055 mmol·L^{-1}. In obese rats, the NEFA reduction was slower despite the comparable drug exposure profiles, and there was no plateau indicative of a lower physiological limit. The lowest measured NEFA concentration in obese rats was 0.16 mmol·L^{-1}.
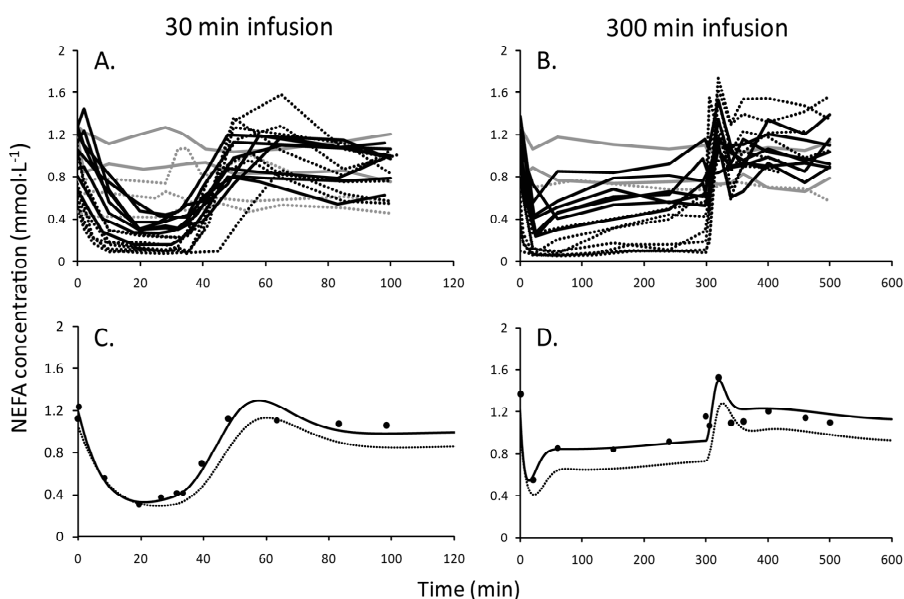

Figure 14. *Plasma NEFA concentration-time profiles during and after infusion of vehicle (grey) or NiAc (black). Observed data for normal (dotted lines) and obese (solid lines) rats (A and B), and predicted data for obese rats (C and D). Control groups received vehicle according to the same regimen as their respective NiAc-treated group. (A) 30 min of 0 or 20 µmol NiAc per kg of body weight; (B) 300 min of 0 or 51 µmol·kg^{-1}. The NEFA concentrations were stable in individual control animals, but there was large variability between animals. Individual (solid line) and population (dotted line) predicted NEFA plasma concentration time-courses in representative obese individuals after (C) 30 min of 20 µmol·kg^{-1} and (D) 300 min of 51 µmol·kg^{-1} NiAc.*

Although NEFA concentrations increased post-infusion in obese rats, they did not exceed the baseline concentration after the 30 min infusions. Rebound and post-rebound oscillations followed the 300 min infusions, but they were substantially less than in the normal rats. There was more pronounced

slowly developing tolerance during the period of constant NiAc exposure in obese than in normal rats, resembling the pattern during 300 min infusions in normal rats at lower NiAc doses (5 or 10 µmol·kg^{-1}, see Figure 12B).

Representative individual and population predictions superimposed on experimental data after different doses and infusion times are shown in Figure 14C and D. Although the pharmacodynamic characteristics in obese and normal rats differed, the new feedback model also described the pattern of NiAc-induced changes in NEFA in the obese rats, capturing the increased NEFA baseline, the pronounced slowly developing tolerance, the diminished rebound, and, following the 300 min infusions, the post-rebound oscillations. However, as the dose was too low, no lower physiological limit of NEFA was reached, so k_{cap} could not be estimated with acceptable precision in the modelling process. When k_{cap} was fixed to the value of the normal rats, the precision in the rest of the parameters was impaired and the OFV increased. It was therefore fixed to zero throughout the analysis.

Table 7. *Summary of qualitative differences between obese and normal rats in NEFA concentration-time profiles, after a 30 min (20 µmol·kg^{-1}) or 300 min (51 µmol·kg^{-1}) intravenous infusion of NiAc*

Pharmacodynamic feature	Obese rats		Normal rats	
	30 min	300 min	30 min	300 min
Rebound	-	+	++	++
Post-rebound oscillations	-	+	-	++
Slow developing tolerance	-	++	-	+
Lower physiological limit	-	-	++	++

+ = observed, ++ = more pronounced, - = not observed

The final population parameter estimates and inter-individual variabilities are shown in Table 6. All primary parameters were estimated with high precision with the exception of IC_{50}. The poor precision in IC_{50} may reflect the large number of parameters and the limited number of animals. Simultaneous analysis of the normal and obese animal data may give estimates with higher precision. Compared to the normal rats (Paper IV), R_0, p and k_{in} (estimated as a secondary parameter in the analysis) were increased by 44, 78 and 41 %, respectively, in the obese rats, and k_{out} and γ were reduced by 64 and 84 %. The k_{tol} and IC_{50} were equal in both rat strains.

Insulin inhibits the formation of NEFA (k_{in}, [124, 125]) and stimulates its loss (k_{out}, [125, 126]). Because the NEFA baseline concentration R_0 is governed by

the ratio of k_{in} to k_{out} in obese rats, an increase in k_{in} coupled to a decrease in k_{out} would have a multiplicative effect in raising R_0. Thus, the reduced influence of insulin on NEFA concentrations in insulin-resistant obese Zucker rats is likely to account for the increased R_0.

The dynamics of the moderator and the response can be compared by expressing the ratio of k_{tol} to k_{out}. This ratio was estimated to be 0.085 and 0.30 mmol L^{-1} in normal and obese rats, respectively. It was predicted that, as this ratio increased, the extent of rebound would decrease (Paper III). This is consistent with the reduced rebound and post-rebound oscillations in the obese rats (Figure 14). The amplification factor p was also increased in the obese rats, which, according to predictions in Paper III, would increase the extent of tolerance. Again, this prediction was fulfilled in the obese rats during the period of constant exposure (Figure 14).

4.4 Concentration-response relationship at equilibrium (Papers I, II, IV and V)

By using a quantitative approach, response time-courses can be translated to corresponding concentration-response relationships at equilibrium, enabling graphical comparison of different compounds binding to the same target. The concentration-response relationships at equilibrium obtained in Papers I, II, IV and V are shown in Figure 15.

There was a sigmoid relationship between the simulated steady state concentration of NiAc (C_{SS}) and NEFA (R_{SS}) in normal animals (Papers I, II and IV), with NEFA decreasing as the concentration of NiAc increased from ~ 0.02 to 0.5 µmol·L^{-1}. At NiAc baseline concentrations (region a in Figure 15), discrepancies between the studies reflected differences in the estimates k_{in} and k_{out}, the ratio of which primarily governed the steady state response (see Appendix A in Paper IV). The discrepancies between the studies are due to differences in the estimates of these parameters. At NiAc concentrations around IC_{50} (b in Figure 15) all parameters affected the steady state response (see Appendix B in Paper IV). At high concentrations (c in Figure 15), the steady state response in Papers II and IV was governed by the ratio of k_{cap} to k_{out} (see Appendix B in Paper IV). In Paper I, however, the absence of k_{cap} reduced this response to zero at high concentrations.

In obese animals, the NEFA concentration decreased progressively with increasing NiAc concentration, with no evident plateau and, compared with normal animals, the curve was shifted upwards and to the right, and was

shallower. The extent of such shifts is important, as they demonstrate the impact of disease at equilibrium and, if ignored, will lead to erroneous dose predictions and, in consequence, poorly designed studies. The steady state response for the obese rats at baseline NiAc concentrations was higher than in normal rats (region a in Figure 15), reflecting the multiplicative effect on the NEFA baseline concentration (R_0) of the increase in k_{in} and decrease in k_{out}. At NiAc concentrations around IC_{50} (b in Figure 15), the steady state response was increased in the obese animals because of the multiplicative effect of the increased k_{in} and decreased k_{out}, together with the increase in p. Because of the different estimates for the sigmoidicity factor ($\gamma = 0.35$ in obese rats and ~ 2 in normal rats), the inhibitory drug mechanism function $I(C_p)$ affected the steady state response throughout the therapeutic concentration interval differently in the two groups (see c in Figure 15 and Equation 11). In short, because of the shallow concentration-response relationship in obese rats, it would be possible to increase the drug concentration considerably without materially changing the NEFA response.
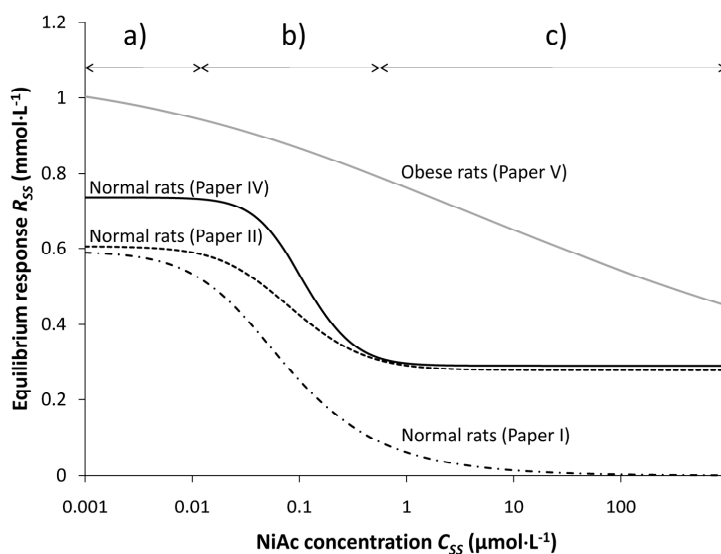

Figure 15. Simulated steady state plasma NiAc concentration (C_{SS}) versus predicted plasma NEFA concentration at equilibrium (R_{SS}) in Papers I (dot-dash black line), II (dashed black line), IV (solid black line) and V (solid grey line). These curves were derived, respectively, using Equations 5, 21 and 23 in Section 3.6.1.1 and 3.6.1.5, and the final parameter estimates in Table 4 (Paper I) and Table 6 (Papers II, IV and V). Regions a, b and c indicate low, intermediate and high NiAc concentrations, respectively.

4.5 Rate and extent of tolerance and rebound (Paper III)

4.5.1 Rate of tolerance development

Infusion and sampling times in any experiment that aims to study tolerance must be sufficiently long to enable tolerance to develop fully. The rate of tolerance development can be addressed by quantitatively estimating the time to steady state, with the time to 90 % of steady state being commonly approximated by 3-4 $t_{1/2}$. The half-life of tolerance development was shown to be dependent on the drug exposure, increasing with increases in drug exposure. Thus, the time to steady state also increased with increased drug exposure.

According to the model, the behaviour of the NiAc-NEFA system at washout is highly dependent on the value of the last moderator. As M_N varies with time, there would be a dynamic input to the loss term of the response, and equilibrium would be established via a damped oscillation.

Here it was found that the time to steady state decreased with increases in k_{tol}/k_{out}. As the ratio of k_{tol} to k_{out} increased, the delay in the moderators responsible for overshoot and rebound would diminish, with the system reaching equilibrium more rapidly. The moderator time-courses would closely follow the response time-course, preventing overshoot and rebound and reducing the time to equilibrium, when the k_{tol} parameter gets large.

4.5.2 Extent of tolerance

The extent of tolerance varies with the type of drug used. This is reflected by the underlying mechanism of tolerance development and results in different patterns of the concentration-response curve [4]. The extent of tolerance can be quantified in various ways, such as alterations in the response time-course at one specific drug exposure or differences in the steady state concentration-response relationship between a tolerant and a non-tolerant system. For a tolerant system, a higher drug exposure would be needed to achieve a specific effect compared to a non-tolerant system (Figure 16).

The extent of tolerance varied with NiAc steady state concentration and was most pronounced at concentrations slightly higher than IC_{50} (Figure 16).
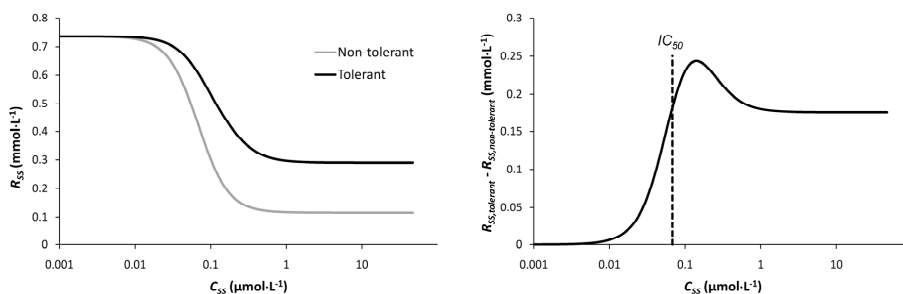
Figure 16. *Simulated steady state plasma NiAc concentration (C_{SS}) versus plasma NEFA concentration (R_{SS}) (left panel) and the difference between the tolerant and non-tolerant steady state relationships (right panel). The black and grey curves in the left panel were derived, respectively, using Equations 12 and 15 in Section 3.6.1.4 and the final parameter estimates obtained in Paper IV (Table 6). The estimate from Paper IV of the potency of NiAc (IC_{50}) is indicated in the right panel.*

4.5.3 Extent of rebound

Too dramatic a rebound may become a safety issue, so if the factors controlling the extent of rebound are known, it is possible they could be used to minimize or even avoid rebound of response. The duration of exposure is one important factor, with rebound being considerably smaller following a short rather than a long drug exposure. According to the feedback model (Figure 6), the moderators counteract the drug-induced changes in the response and, if the drug effect is rapidly removed, there will be a delay before the counteracting effects decline. During short drug exposure (*e.g.* 30 min), M_8 would remain at baseline and have no effect on NEFA concentrations. Thus, when the drug effect was removed, M_1 would be the only moderator pushing the NEFA concentration above baseline. During extended exposure (> 150 min) both M_1 and M_8 would counteract the NiAc-induced reduction in NEFA concentrations, increasing the extent of rebound after abrupt drug removal. These predictions were confirmed experimentally (Figure 8 and Figure 12).

In addition to the duration of exposure, the half-life of a drug influences the magnitude of rebound [18, 20, 22], with rapidly eliminated compounds being accompanied by greater rebound than more slowly eliminated compounds. When the response time-course was simulated following prolonged (2000 min) infusion of a compound with a half-life of 90 min, rebound had almost disappeared compared with that for a compound with a 2 min half-life (Figure 17). In other words, the slow washout kinetics of the drug became the rate-limiting step of the system.

Finally, the model predicts that the underlying cause of rebound is the delayed action of the moderators. This means that the length of the delay, which is governed by the ratio k_{tol}/k_{out}, will be important in determining the extent of rebound. A small ratio would result in a long delay and pronounced rebound; conversely, a large ratio, with its fast moderator dynamics and moderators that closely followed the response, would not lead to rebound. The amplification factor p, intensifies the impact of M_1 on the formation of response (Equation 12). Thus, an increase in p will also result in increased rebound.
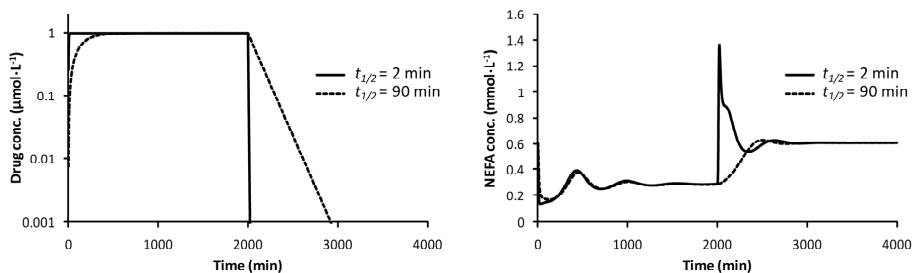

Figure 17. *Simulations of drug disposition and NEFA response during and after a 2000 min infusion of compounds with different half-lives. The drug and system parameters were taken from Paper II (Table 6), using a half-life of 2 min (solid lines) and 90 min (dashed lines). Disposition was assumed to follow mono-exponential elimination. The responses were almost identical during drug exposure but at washout there was no or very little rebound for the more stable compound.*

5   *General discussion*

The aim of these studies was to find a model that looked specifically at acute activation by NiAc of the GPR109A receptor, rather than one that captured all processes involved in NEFA regulation. The reason for this was that acute NiAc-induced changes in NEFA provided a tool for investigating the key determinants of tolerance and rebound in normal and diseased rats. Consequently, there is no attempt to evaluate regulation of the GPR109A/NEFA system on a chronic basis, or to model or consider other receptors which influence plasma NEFA concentrations (*e.g.* adenosine receptors [23, 24] and GPR43 [149]). By using a quantitative approach restricted to the acute activation of the NiAc-NEFA system it was possible to investigate whether NiAc-induced tolerance and rebound, with their associated risks, could be avoided. Consequently, the existence and pattern of tolerance and rebound are stressed throughout this thesis.

The NiAc-NEFA system was selected as a tool-system in these studies because of the short half-life of NiAc, the rapid onset and offset of the NiAc-induced changes in NEFA, and the fact that the NEFA response manifests tolerance and rebound. Not only do changes in NEFA plasma concentration in rats commence within 5 min of initiating NiAc infusion, but steady state exposure to NiAc is reached within 10 min and the decline of NiAc exposure is rapid, facilitating the study of potential rebound [17-22, 107].

The NEFA tolerance cannot be explained by changes in drug pharmaco-kinetics, as the steady state plasma concentrations remain constant during the NiAc infusions [45, 150]. Thus, the NEFA tolerance was classified as functional tolerance, which is defined as the reduction of drug-induced effect in the presence of the same drug concentration [4, 46, 87, 89-93]. This phenomenon may arise from down-regulation or alterations of receptor populations, depletion of endogenous intermediaries or from homeostatic counteracting mechanisms [66, 151, 152]. Throughout this thesis, the NEFA tolerance and rebound are assumed to be caused by endogenous counter-

acting mechanisms that are integrated in a moderator. The formation of the moderator is driven by the NEFA concentration. These assumptions appeared to be physiologically relevant as insulin, glucose, glucagon, growth hormone, cortisol and TG are known to be involved in the NEFA regulation [124-126, 153-155].

In Paper I, an inventory of previously performed rat experiments was carried out and a dose-response-time model was fitted to the response-time data in the absence of measured NiAc exposure. This approach often requires a wider dose range, multiple dosing, a longer observational period, pharmaco-dynamic sampling at optimal time points and/or a larger number of subjects than is the case for exposure-driven approaches to modelling [96, 140]. The experimental design incorporated several provocations, providing a good basis for dose-response-time modelling. The model was based on a previously published feedback model [22, 103-107] in which feedback was described by means of an endogenous moderator that counteracted the changes in response. Because the model captured the experimental data consistently it was used for the design of the next set of experiments, which investigated tolerance and rebound in the NiAc-NEFA system in normal rats.

The study outlined in Paper II revealed new information, with tolerance being seen as increasing NEFA concentrations in the presence of constant NiAc exposure and the extent of rebound being dependent on both the level and duration of drug exposure. In addition, there were rebound oscillations following long duration NiAc exposure. This non-intuitive pattern was captured by a new feedback model with a moderator distributed over a series of transit compartments, where the level of moderator in the first compartment inhibited the formation of response and that in the last compartment stimulated the loss of response. The model was based on mechanistic principles, mimicking the dual actions of insulin in inhibiting the hydrolysis of NEFA to TG and glycerol [124, 125] and stimulating the re-esterification of NEFA [125, 126]. NiAc-induced reduction of NEFA followed by a substantial rebound has been reported in mice, rats, dogs and humans [15, 16, 50, 146, 156-158]. However, to our knowledge oscillations in the rebound following extended exposure has not previously been reported.

Although NiAc is primarily administered orally in daily doses of 1.5-3 g [58] in the clinic, it was infused in the experiments in Paper II. In Paper IV, the new model was therefore challenged further. Firstly, different oral doses of NiAc were used to elicit NEFA response-time data, and secondly, the impact on the extent of rebound was evaluated by decreasing the rate at which

exposure declined. The model captured the NEFA response following all the provocations and different patterns of NiAc exposure. Now that the model has been challenged successfully by different rates and routes of administration, and its system parameters have been estimated with high certainty, it may be possible to carry out simulations using other dose regimens, and to scale the parameters to other species.

The model developed in Paper II and challenged in Paper IV was novel. In order to understand its characteristics and the features that enabled it to describe NiAc-induced changes in NEFA, it was analyzed mathematically in Paper III. Here it was shown that the rate of tolerance and time to pharmacodynamic steady state were dependent on drug exposure, with the half-life of the response being increased with increasing drug exposure, approximating 300-400 min at high exposure ($I(C_p) \approx 0$). For the simpler feedback model used in Paper I, the half-life of response was independent of drug exposure and substantially shorter. Although the duration of the extended (300 min) infusion experiments in Papers II and IV, was selected on the basis of the Paper I model, it was intended to be sufficient for the system to reach steady state. However, quantitative analysis using the full model predicted that the time to steady state would be substantially longer than this and that it would be dependent on drug exposure. In fact, an infusion of 25 h would be required for the system to reach pharmacodynamic steady state irrespective of drug exposure (see Appendix C in Paper III). In addition to drug exposure, the rate of tolerance is a multifactorial process governed not only by the slowest rate constant (*e.g.* if $k_{tol} < k_{out}$), but also by the disequilibrium between R and M.

The extent of tolerance was primarily determined by the steady state drug concentration C_{ss}, being most pronounced at concentrations slightly higher than IC_{50}. However, tolerance also increased as the ratio of k_{tol} to k_{out} decreased. The extent of rebound was primarily governed by the duration of drug exposure and its rate of reduction. To minimize rebound, a slow decrease in drug exposure is needed primarily at drug concentrations around IC_{50}. Such information is vital when optimizing the properties of NiAc analogues.

Because the presence of underlying disease may alter the kinetics of drug action [3, 110-117], its impact on the response to a drug must be evaluated for successful translation to patients. In Paper V, NiAc was given to obese Zucker rats, a disease model of dyslipidaemia and insulin resistance [127-129, 159]. This provided a further challenge to the newly proposed feedback

model. The pharmacodynamic characteristics in the diseased and normal animals differed, with NEFA baseline concentrations being increased, rebound being diminished, and tolerance development being more pronounced in the obese rats. This resulted in a concentration-response relationship at steady state that was shifted upwards and to the right, and was shallower, than that for normal animals. The extent of such shifts is important, as they demonstrate the impact of disease at equilibrium and, if ignored, will lead to erroneous dose predictions and, as a consequence, poorly designed studies. Obviously it would require future studies in healthy and patient populations to evaluate the performance of the model in the clinic.

Although, NiAc is an effective and unique anti-lipolytic agent, unwanted effects such as cutaneous vasodilation evident as flushing, and rebound, reduce its therapeutic usefulness [58, 160-164]. Furthermore, its intrinsic characteristics mean that variations in the dose regimen are less likely to prevent rebound. In spite of this, it was considered important to estimate the NiAc-NEFA system parameters in these studies because, by means of the system properties, it will be possible to simulate response time-courses for NiAc analogues with different drug parameter estimates. The purpose of such simulations would be to find a potential compound that could be taken prior to a meal, elicit a rapid and substantial decrease in NEFA lasting around 2 h, and would not produce rebound. With reduced NEFA concentration, glucose will be used as a source of energy which may eventually result in improved insulin sensitivity [38-40]. Short effect duration has proven to be beneficial for systems exhibiting tolerance, as the primary effect does not last long enough for the counteracting mechanisms, accountable for tolerance and rebound, to develop [42-47]. The results of the present studies support the proposition that a compound which fulfilled these requirements and satisfied appropriate properties in terms of its pharmacokinetics, potency, efficacy and sigmoidicity, should be targeted. The compound should also not give rise to flushing. Although the present studies made no attempt to evaluate the relationship between NiAc exposure and flushing because of the extensive nature of such experiments, establishing such a relationship would greatly facilitate the development of a clinically useful NiAc analogue.

By designing studies that looked at the consequences of changing the rate and route of administration of NiAc, and the duration of its exposure, and by coupling these data to washout dynamics, it has been possible to reveal and better understand the development and magnitude of tolerance and

rebound. However, to ensure that the model adequately captures the response before, during and after pharmacodynamic steady state, studies are needed where NiAc and NiAc analogues are infused for at least 25 h. Finally, although the current experiments in obese rats evaluated the kinetics of drug action in a diseased state, they provided no information about the effect on disease progression. To obtain such data it would be valuable to follow disease progression in untreated genetically obese Zucker rats over several months, monitoring NEFA, insulin, glucose, TG, growth hormone, cortisol and glucagon [124-126, 153-155]. Initiating and terminating treatment with NiAc or a NiAc analogue at different stages of the disease would then reveal any effect of the drug on disease progression [165].

In conclusion, these studies have highlighted not only examples of drug properties that can be revealed by models based on mechanistic principles, but also the inherent value of such modelling in pharmaceutical discovery and development.

6 Conclusions

The overall aim of this thesis was to study tolerance and rebound in normal and diseased rats, using nicotinic acid (NiAc)-induced changes in non-esterified fatty acids (NEFA) as a tool-system. The work described in this thesis comprises studies in Sprague Dawley (normal) and obese Zucker (diseased) rats who were given NiAc as intravenous infusions in doses of 1-51 μmol$\cdot$kg^{-1} over 30-300 min, or as oral doses of 24-810 μmol$\cdot$kg^{-1}. These NiAc doses reduced NEFA concentration in plasma to approximately 10 % of the predose baseline level. The results obtained allow the following conclusions regarding the pharmacokinetics and pharmacodynamics of the NiAc-NEFA system:

- A dose-response-time model with feedback included as a moderator that inhibits the formation of response, described the NiAc-induced changes in NEFA plasma concentrations in absence of measured drug exposure

- The dose-response-time model could be used for design of new experiments, but the model under-predicted the time to pharmaco-dynamic steady state

- A two-compartment model with two parallel capacity-limited elimination pathways described the NiAc disposition adequately in normal rats

- The absorption of NiAc from the gastrointestinal tract in normal rats could be described by a linear and a non-linear process

- A one-compartment model with a single capacity-limited elimination pathway, described the NiAc disposition in diseased animals, but the inter-individual variabilities were estimated with low precision

- Different rates and routes of NiAc administration to normal rats revealed a slowly developing tolerance in spite of constant drug exposure, a substantial rebound that oscillated following long duration of NiAc exposure and a lower physiological limit in NEFA concentrations

- The lower physiological limit seen in normal rats was modelled as a zero-order production term k_{cap} of NEFA representing the lipoprotein lipase-catalyzed hydrolysis of TG to NEFA and glycerol in the capillaries

- A model with feedback governed by a series of transit compartments, where the moderator in the first and last compartment inhibits the formation and stimulates the loss of response, respectively, described the tolerance and oscillatory rebound seen in normal rats

- NEFA rebound was diminished and the slowly developing tolerance was more pronounced in diseased rats compared to normal rats

- No lower physiological limit was observed in the diseased rats at drug exposure levels comparable to the ones in normal rats

- The feedback model with a series of moderators also captured the altered pharmacodynamic characteristics seen in diseased rats

- Compared to the normal rats the k_{in}, p and R_0 were increased by 41, 78 and 44 %, respectively, in the diseased rats, and k_{out} and γ were reduced by 64 and 84 %. The k_{tol} and IC_{50} were equal in both physiological states (normal/diseased)

- The concentration-response relationship in normal rats was steep, with NEFA decreasing as NiAc increased from 0.02-0.5 µmol·L^{-1}

- The concentration-response relationship in diseased animals was shifted upwards and to the right, and was more shallow than that for the normal animals

- The rate of tolerance development is dependent on the drug concentration and on the dynamics of the moderators (k_{tol}) relative to the dynamics of response (k_{out})

- The extent of tolerance is determined by the steady state drug concentration and the dynamics of the moderators (k_{tol}) relative to the dynamics of response (k_{out})

- The extent of rebound is primarily governed by the duration and decline of drug exposure

- A study design with different durations, rates and routes of drug administration coupled to washout dynamics, has shown to be critical to reveal and better understand the development and magnitude of tolerance and rebound

7   Populärvetenskaplig sammanfattning

Tolerans är när effekten av ett läkemedel avtar trots att halten av läkemedel i blodet är oförändrad. Toleransutveckling följs ibland av en reboundeffekt, vilket innebär att när läkemedlet försvunnit ur kroppen uppkommer, för en tid, en effekt som är motsatt den positiva effekt som läkemedlet hade. Både tolerans och reboundeffekt är oönskade egenskaper hos ett läkemedel. Om man förstår vilka biologiska mekanismer som orsakar tolerans och rebound-effekt kan man eventuellt hitta ett läkemedel och en doseringsform där dessa oönskade effekter kan undvikas.

Nikotinsyra är ett läkemedel som sänker fria fettsyror i blodet. Om halten nikotinsyra i blodet hålls konstant kan man se toleransutveckling som en liten ökning av halten fettsyror i blodet över tiden. När en behandling med nikotinsyra avslutas ökar halten fettsyror i blodet fort och når halter högre än den ursprungliga nivån. Detta är vad vi kallar en reboundeffekt. I detta avhandlingsarbete används nikotinsyras sänkning av fettsyror i friska och sjuka råttor som ett modellsystem för att studera och få bättre kunskap om vad som kan orsaka tolerans och rebound och hur man eventuellt kan undkomma dessa problem.

Förändringen i halten fettsyror vid behandling med nikotinsyra skiljde sig åt mellan friska och sjuka råttor. Nivån av fettsyror i blodet innan behandlingen påbörjades var högre i de sjuka djuren än i de friska. Man kunde inte heller sänka nivån av fettsyror lika mycket i de sjuka djuren som i de friska. Efter behandlingen avslutades var reboundeffekten i de sjuka djuren mycket mindre än i de friska. Genom att bygga in denna information i en matematisk modell kunde de oväntade resultaten förklaras.

Med en modell som beskriver den biologiska verkningsmekanismen hos ett läkemedel kan effekten av läkemedlet efter olika typer av doseringsformer förutsägas. Modellen kan även användas för att förutsäga hur effekten skulle se ut i andra djurslag och slutligen i människa.

Sammanfattningsvis kan sägas att detta avhandlingsarbete ökat förståelsen för hur viktig doseringsformen av ett läkemedel är för att man ska upptäcka toleransutveckling och reboundeffekt. Effekten av ett läkemedel, tolerans-utveckling och rebound kan skilja sig mycket mellan friska och sjuka individer. Detta måste man studera och ta hänsyn till när man bedömer användbarheten och bestämmer doseringsformen av ett läkemedel i patienter.

8 Acknowledgements

A special thanks to my family. Mum and dad, thank you for everything. You are the best! I would not have been here without your constant support. Lotta, Fredrik, Niclas, Krystle, Oskar and Gustav for always being there to listen and to cheer me up. I have constantly felt your support!

Urban, for always having patience with my black or white personality and for always turning bad to good. No one makes me feel as good as you. You are my everything!

9 References

1. Holford N.H.G., Sheiner L.B. Kinetics of pharmacologic response. *Pharmacol. Ther.* **1982.** 16(2): 143-166

2. Levy G. Kinetics of drug action: an overview. *J. Allergy. Clin. Immunol.* **1986.** 78: 754-761

3. Levy G. The case for preclinical pharmacodynamics. In: Integration of Pharmacokinetics, Pharmacodynamics and Toxicokinetics in Rational Drug Development, Ed. Yacobi A., Shah V., Skelly J. and Benet L., Plenum Press, New York. **1993.** pp. 7-13

4. Kalant H., LeBlanc A.E., Gibbins R.J. Tolerance to, and dependence on, some non-opiate psychotropic drugs. *Pharmacol. Rev.* **1971.** 33(3): 135-191

5. Weber S., Auclert L., Touiza K., Pellois A., Guerin C., Blin P., Guerin F. Evaluation of tolerance during intravenous administration of low dose of isosorbide dinitrate in the treatment of unstable angina. *Arch. Mal. Coeur. Vaiss.* **1992.** 85(1): 59-65

6. Miyata H., Yanagita T. Mechanism of nicotine dependence. *Jpn. J. Alc. Stud. Drug Depend.* **1998.** 33(5): 557-573

7. Lader M. The consequences of zopiclone use: Rebound insomnia, development of tolerance, and abuse potential. *Rev. Contemp. Pharmacother.* **1998.** 9(2): 131-140

8. Hancox R.J., Cowan J.O., Flannery E.M., Herbison G.P., Mclachlan C.R., Taylor D.R. Bronchodilator tolerance and rebound bronchoconstriction during regular inhaled beta-agonist treatment. *Respir. Med.* **2000.** 94(8): 767-771

9.   Schwemmer M., Bassenge E. New approaches to overcome tolerance to nitrates. *Cardiovasc. Drugs Ther.* **2003.** 17(2): 159-173

10.   Anand K.J., Willson D.F., Berger J., Harrison R., Meert K.L., Zimmerman J., Carcillo J., Newth C.J.L., Prodhan P., Dean J.M., Nicholson C. Tolerance and withdrawal from prolonged opioid use in critically ill children. *Pediatrics.* **2010.** 125(5): 1208-1225

11.   Roegler C., Konig A., Glusa E., Lehmann J. A novel class of nitrovasodilators: potency and in vitro tolerance of organic aminoalkylnitrates. *J Cardiovasc Pharmacol.* **2010.** 56(5): 484-490

12.   Canner P.L., Berge K.G., Wenger N.K. Fifteen year mortality in Coronary Drug Project patients: Long-term benefit with niacin. *J. Am. Coll. Cardiol.* **1986.** 8(6): 1245-1255

13.   Carlson L.A., Rosenhamer G. Reduction of mortality in the Stockholm ischaemic heart disease secondary prevention study by combined treatment with clofibrate and nicotinic acid. *Acta. Med. Scand.* **1988.** 223(5): 405-418

14.   Carlson L.A. Nicotinic acid: The broad-spectrum lipid drug. A 50th anniversary review. *J. Intern. Med.* **2005.** 258(2): 94-114

15.   Carlson L.A., Orö L. The effect of nicotinic acid on the plasma free fatty acid: demonstration of a metabolic type of sympathicolysis. *Acta. Med. Scand.* **1962.** 172: 641-645

16.   Carlson L.A. Studies on the effect of nicotinic acid on catecholamine stimulated lipolysis in adipose tissue in vitro. *Acta. Med. Scand.* **1963.** 173: 719-722

17.   Fontaine R., Chouinard G., Annable L. Rebound anxiety in anxious patients after abrupt withdrawal of benzodiazepine treatment. *Am. J. Psychiatry.* **1984.** 141(7): 848-852

18.   Bixler E.O., Kales J.D., Kales A., Jacoby J.A., Soldatos C.R. Rebound insomnia and elimination half-life: assessment of individual subject response. *J. Clin. Pharmacol.* **1985.** 25(2): 115-124

19.   Cantopher T., Olivieri S., Cleave N., Edwards J.G. Chronic benzodiazepine dependence. A comparative study of abrupt

withdrawal under propranolol cover versus gradual withdrawal. *Br. J. Psychiatry.* **1990.** 156: 406-411

20.   Bauer J.A., Fung H.L. Effect of apparent elimination half-life on nitroglycerin-induced hemodynamic rebound in experimental heart failure. *Pharm. Res.* **1993.** 10(9): 1341-1345

21.   Dallal A., Chouinard G. Withdrawal and Rebound Symptoms Associated With Abrupt Discontinuation of Venlafaxine. *J. Clin. Psychopharmacol.* **1998.** 18(4): 343-344

22.   Gabrielsson J., Peletier L.A. A nonlinear feedback model capturing different patterns of tolerance and rebound. *Eur. J. Pharm. Sci.* **2007.** 32(2): 85-104

23.   van Schaick E.A., De Greef H.J., Ijzerman A.P., Danhof M. Physiological indirect effect modeling of the antilipolytic effects of adenosine A1-receptor agonists. *J. Pharmacokinet. Biopharm.* **1997.** 25(6): 673-694

24.   van der Graaf P.H., van Schaick E.A., Visser S.A.G., De Greef H.J., Ijzerman A.P., Danhof M. Mechanism-based pharmacokinetic-pharmacodynamic modeling of antilipolytic effects of adenosine A(1) receptor agonists in rats: prediction of tissue-dependent efficacy in vivo. *J. Pharmacol. Exp. Ther.* **1999.** 290(2): 702-709

25.   Ballantyne C.M., O'Keefe J.H., Gotto A.M. Overview of Atherosclerosis and Dyslipidemia. In: Dyslipidemia & Atherosclerosis Essentials, Jones and Bartlett Publishers, Sudbury, MA, USA. **2009.** pp. 1-16

26.   National Cholesterol Education Program. Detection, Evaluation and Treatment of High Blood Cholesterol in Adults. **2002.** http://www.nhlbi.nih.gov/guidelines/cholesterol/atp3full.pdf

27.   Cardiovascular diseases. WHO. Fact Sheet No. 317. **2009.** http://www.who.int/mediacentre/factsheets/fs317/en/index.html

28.   Grundy S.M., Mok H.Y.I., Zech L., Berman M. Influence of nicotinic acid on metabolism of cholesterol and triglycerides in man. *J. Lipid Res.* **1981.** 22(1): 24-36

29. Vega G.L., Grundy S.M. Lipoprotein responses to treatment with lovastatin, gemfibrozil, and nicotinic acid in normolipidemic patients with hypoalphalipoproteinemia. *Arch. Intern. Med.* **1994.** 154(1): 73-82

30. Martin-Jadraque R., Tato F., Mostaza J.M., Vega G.L., Grundy S.M. Effectiveness of low-dose crystalline nicotinic acid in men with low high-density lipoprotein cholesterol levels. *Arch. Intern. Med.* **1996.** 156(10): 1081-1088

31. Mostaza J.M., Schulz I., Vega G.L., Grundy S.M. Comparison of pravastatin with crystalline nicotinic acid monotherapy in treatment of combined hyperlipidemia. *Am. J. Cardiol.* **1997.** 79(9): 1298-1301

32. Guyton J.R., Goldberg A.C., Kreisberg R.A., Sprecher D.L., Superko H.R., O'Connor C.M. Effectiveness of once-nightly dosing of extended-release niacin alone and in combination for hypercholesterolemia. *Am. J. Cardiol.* **1998.** 82(6): 737-743

33. Knopp R.H., Alagona P., Davidson M., Goldberg A.C., Kafonek S.D., Kashyap M., Sprecher D., Superko H.R., Jenkins S., Marcovina S. Equivalent efficacy of a time-release form of niacin (Niaspan) given once-a-night versus plain niacin in the management of hyperlipidemia. *Metab. Clin. Exp.* **1998.** 47(9): 1097-1104

34. Capuzzi D.M., Guyton J.R., Morgan J.M., Goldberg A.C., Kreisberg R.A., Brusco O.A., Brody J. Efficacy and safety of an extended-release niacin (Niaspan): a long-term study. *Am. J. Cardiol.* **1998.** 82(12): 74-81

35. Guyton J.R., Blazing M.A., Hagar J., Kashyap M.L., Knopp R.H., McKenney J.M., Nash D.T., Nash S.D. Extended-release niacin vs gemfibrozil for the treatment of low levels of high-density lipoprotein cholesterol. *Arch. Intern. Med.* **2000.** 160(8): 1177-1184

36. Wilkins R.W., Bearman J.E., Boyle E., Smith W.M., Stamler J. Clofibrate and niacin in coronary heart disease. *J. Am. Med. Assoc.* **1975.** 231(27): 360-381

37. Tavintharan S., Kashyap M.L. The benefits of niacin in atherosclerosis. *Curr. Atheroscler. Rep.* **2001.** 3(1): 74-82

38. Fulcher G.R., Walker M., Catalano C., Agius L., Alberti K.G.M.M. Metabolic effects of suppression of nonesterified fatty acid levels with acipimox in obese NIDDM subjects. *Diabetes.* **1992.** 41(11): 1400-1408

39. Kumar S., Durrington P.N., Bhatnagar D., Laing I. Suppression of non-esterified fatty acids to treat type A insulin resistance syndrome. *Lancet.* **1994.** 343(8905): 1073-1074

40. Bajaj M., Suraamornkul S., Kashyap S., Cusi K., Mandarino L., DeFronzo R.A. Sustained reduction in plasma free fatty acid concentration improves insulin action without altering plasma adipocytokine levels in subjects with strong family history of type 2 diabetes. *J. Clin. Endocrinol. Metab.* **2004.** 89(9): 4649-4655

41. Garg A., Grundy S.M. Nicotinic acid as therapy for dyslipidemia in non-insulin-dependent diabetes mellitus. *J. Am. Med. Assoc.* **1990.** 264(6): 723-726

42. Thadani U., Ho Leung Fung Darke A.C., Parker J.O. Oral isosorbide dinitrate in angina pectoris: Comparison of duration of action and dose-response relation during acute and sustained therapy. *Am. J. Cardiol.* **1982.** 49(2): 411-419

43. Jamrozik K., Fowler G., Vessey M., Wald N. Placebo controlled trial of nicotine chewing gum in general practice. *Br. Med. J.* **1984.** 289(6448): 794-797

44. Parker J.O., Fung H.L. Transdermal nitroglycerin in angina pectoris. *Am. J. Cardiol.* **1984.** 54(6): 471-476

45. Jordan R.A., Seth L., Casebolt P. Rapidly developing tolerance to transdermal nitroglycerin in congestive heart failure. *Ann. Intern. Med.* **1986.** 104(3): 295-298

46. Elkayam U., Kulick D., McIntosh N. Incidence of early tolerance to hemodynamic effects of continuous infusion of nitroglycerin in patients with coronary artery disease and heart failure. *Circulation.* **1987.** 76(3): 577-584

47.   Porchet H.C., Benowitz N.L., Sheiner L.B. Pharmacodynamic model of tolerance: Application to nicotine. *J. Pharmacol. Exp. Ther.* **1988.** 244(1): 231-236

48.   Altschul R., Hoffer A., Stephen J. Influence of nicotinic acid on serum cholesterol in man. *Arch. Biochem. Biophys.* **1955.** 54: 558-559

49.   Soga T., Kamohara M., Takasaki J., Matsumoto S.I., Saito T., Ohishi T., Hiyama H., Matsuo A., Matsushime H., Furuichi K. Molecular identification of nicotinic acid receptor. *Biochem. Biophys. Res. Commun.* **2003.** 303(1): 364-369

50.   Tunaru S., Kero J., Schaub A., Wufka C., Blaukat A., Pfeffer K., Offermanns S. PUMA-G and HM74 are receptors for nicotinic acid and mediate its anti-lipolytic effect. *Nat. Med.* **2003.** 9(3): 352-355

51.   Wise A., Foord S.M., Fraser N.J., Barnes A.A., Elshourbagy N., Eilert M., Ignar D.M., Murdock P.R., Steplewski K., Green A., Brown A.J., Dowell S.J., Szekeres P.G., Hassalli D.G., Marshall F.H., Wilson S., Pike N.B. Molecular identification of high and low affinity receptors for nicotinic acid. *J. Biol. Chem.* **2003.** 278(11): 9869-9874

52.   Carlson L.A., Hanngren A. Initial distribution in mice of ^{3}H-labeled nicotinic acid studied with autoradiography. *Life Sci.* **1964.** 3: 867-871

53.   Butcher R.W., Baird C.E., Sutherland E.W. Effects of lipolytic and antilipolytic substances on adenosine 3',5'-monophosphate levels in isolated fat cells. *J. Biol. Chem.* **1968.** 243(8): 1705-1712

54.   Aktories K., Schultz G., Jakobs K.H. Regulation of adenylate cyclase activity in hamster adipocytes. Inhibition by prostaglandins, alpha-adrenergic agonists and nicotinic acid. *Naunyn Schmiedebergs Arch. Pharmacol.* **1980.** 312(2): 167-173

55.   Sprecher D.L. Raising high-density lipoprotein cholesterol with niacin and fibrates: a comparative review. *Am. J. Cardiol.* **2000.** 86(12): 46-50

56.   Le Goff W., Guerin M., Chapman M.J. Pharmacological modulation of cholesteryl ester transfer protein, a new therapeutic target in atherogenic dyslipidemia. *Pharmacol. Ther.* **2004.** 101(1): 17-38

57. Gibbons L.W., Gonzalez V., Gordon N., Grundy S. The prevalence of side effects with regular and sustained-release nicotinic acid. *Am. J. Med.* **1995.** 99(4): 378-385

58. Offermanns S. The nicotinic acid receptor GPR109A (HM74A or PUMA-G) as a new therapeutic target. *Trends. Pharmacol. Sci.* **2006.** 27(7): 384-390

59. Colpaert F.C. Drug discrimination: No evidence for tolerance to opiates. *Pharmacol. Rev.* **1995.** 47(4): 605-629

60. Benowitz N.L. Tolerance as a modulator of drug response. In: Variability in Human Drug Response, Ed. Tucker G.T., Elsevier Science B.V., **1999.** pp. 93-108

61. Fowler S.C. Behavioral tolerance (contingent tolerance) is mediated in part by variations in regional cerebral blood flow. *Brain Mind.* **2000.** 1(1): 45-57

62. Gresch P.J., Smith R.L., Barrett R.J., Sanders-Bush E. Behavioral tolerance to lysergic acid diethylamide is associated with reduced serotonin-2A receptor signaling in rat cortex. *Neuropsychopharmacology.* **2005.** 30(9): 1693-1702

63. Le A.D., Poulos C.X., Cappell H. Conditioned tolerance to the hypothermic effect of ethyl alcohol. *Science.* **1979.** 206(4422): 1109-1110

64. Melchior C.L. Conditioned tolerance provides protection against ethanol lethality. *Pharmacol. Biochem. Behav.* **1990.** 37(1): 205-206

65. Ehrman R., Ternes J., O'Brien C.P., McLellan A.T. Conditioned tolerance in human opiate addicts. *Psychopharmacology.* **1992.** 108(1-2): 218-224

66. Insel P.A. Adrenergic receptors - Evolving concepts and clinical implications. *N. Engl. J. Med.* **1996.** 334(9): 580-585

67. Wolfe R.M. Antidepressant withdrawal reactions. *Am. Fam. Physician.* **1997.** 56(2): 455-462

68. Oniani T.N., Akhvlediani G.R. Influence of some monoamine oxidase inhibitors on the sleep-wakefulness cycle of the cat. *Neurosci. Behav. Physiol.* **1988.** 18(4): 301-306

69. Borrelli B., Spring B., Niaura R., Kristeller J., Ockene J.K., Keuthen N.J. Weight suppression and weight rebound in ex-smokers treated with fluoxetine. *J. Consult. Clin. Psychol.* **1999.** 67(1): 124-131

70. D'Aquila P.S., Panin F., Serra G. Long-term imipramine withdrawal induces a depressive-like behaviour in the forced swimming test. *Eur. J. Pharmacol.* **2004.** 492(1): 61-63

71. Huang X.F., Han M., Huang X., Zavitsanou K., Deng C. Olanzapine differentially affects 5-HT2A and 2C receptor mRNA expression in the rat brain. *Behav. Brain Res.* **2006.** 171(2): 355-362

72. Hodding G.C., Jann M., Ackerman I.P. Drug withdrawal syndromes - a literature review. *West. J. Med.* **1980.** 133(5): 383-391

73. Williams B.A., Bottegal M.T., Kentor M.L., Irrgang J.J., Williams J.P. Rebound pain scores as a function of femoral nerve block duration after anterior cruciate ligament reconstruction: Retrospective analysis of a prospective, randomized clinical trial. *Reg. Anesth. Pain. Med.* **2007.** 32(3): 186-192

74. Rangno R.E., Langlois S. Comparison of withdrawal phenomena after propranolol, metoprolol, and pindolol. *Am. Heart J.* **1982.** 104(2): 473-478

75. Egstrup K. Transient myocardial ischemia after abrupt withdrawal of antianginal therapy in chronic stable angina. *Am. J. Cardiol.* **1988.** 61(15): 1219-1222

76. Ferratini M. Risk of rebound phenomenon during nitrate withdrawal. *Int. J. Cardiol.* **1994.** 45(2): 89-96

77. Fung H.L., Bauer J.A. Mechanisms of nitrate tolerance. *Cardiovasc. Drugs Ther.* **1994.** 8(3): 489-499

78. Watanabe H., Kakihana M., Ohtsuka S., Sugishita Y. Efficacy and rebound phenomenon related to intermittent nitroglycerin therapy

for the prevention of nitrate tolerance. *Jpn. Circ. J.* **1998.** 62(8): 571-575

79. Hebert D., Lam J.Y.T. Nitroglycerin rebound associated with vascular, rather than platelet, hypersensitivity. *J. Am. Coll. Cardiol.* **2000.** 36(7): 2311-2316

80. Goodman and Gilman's The Pharmacological Basis of Therapeutics. 9th ed. The McGraw-Hill Companies, Inc., New York, **1996.**

81. Bauer J.A., Fung H.L. Pharmacodynamic models of nitroglycerin-induced hemodynamic tolerance in experimental heart failure. *Pharm. Res.* **1994.** 11(6): 816-823

82. Aarons R.D., Nies A.S., Gal J. Elevation of beta-adrenergic receptor density in human lymphocytes after propranolol administration. *J. Clin. Invest.* **1980.** 65(5): 949-952

83. Ross P.J., Lewis M.J., Sheridan D.J., Henderson A.H. Adrenergic hypersensitivity after beta-blocker withdrawal. *Br. Heart J.* **1981.** 45(6): 637-642

84. Gabrielsson J., Weiner D. Pharmacokinetic and Pharmacodynamic Data Analysis: Concepts and Applications. 4th ed. Swedish Pharmaceutical Press, Stockholm, **2006.**

85. Russell M.A., Feyerabend C. Cigarette smoking: a dependence on high-nicotine boli. *Drug Metab. Rev.* **1978.** 8(1): 29-57

86. Rosenberg J., Benowitz N.L., Jacob P., Wilson K.M. Disposition kinetics and effects of intravenous nicotine. *Clin. Pharmacol. Ther.* **1980.** 28(4): 517-522

87. Kroboth P.D., Smith R.B., Erb R.J. Tolerance to alprazolam after intravenous bolus and continuous infusion: Psychomotor and EEG effects. *Clinical Pharmacology & Therapeutics.* **1988.** 43(3): 270-277

88. Shi J., Benowitz N.L., Denaro C.P., Sheiner L.B. Pharmacokinetic-pharmacodynamic modeling of caffeine: Tolerance to pressor effects. *Clin. Pharmacol. Ther.* **1993.** 53(1): 6-14

89.   Kroboth P.D., Bertz R.J., Smith R.B. Acute tolerance to triazolam during continuous and step infusions: Estimation of the effect offset rate constant. *J. Pharmacol. Exp. Ther.* **1993.** 264(3): 1047-1055

90.   Unverferth D.V., Blanford M., Kates R.E., Leier C.V. Tolerance to dobutamine after a 72 hour continuous infusion. *Am. J. Med.* **1980.** 69(2): 262-266

91.   Zimrin D., Reichek N., Bogin K.T., Aurigemma G., Douglas P., Berko B., Fung H.L. Antianginal effects of intravenous nitroglycerin over 24 hours. *Circulation.* **1988.** 77(6): 1376-1384

92.   Kissin I., Brown P.T., Robinson C.A., Bradley E.L. Jr. Acute tolerance in morphine analgesia: Continuous infusion and single injection in rats. *Anesthesiology.* **1991.** 74(1): 166-171

93.   Fattinger K., Verotta D., Benowitz N.L. Pharmacodynamics of acute tolerance to multiple nicotinic effects in humans. *J. Pharmacol. Exp. Ther.* **1997.** 281(3): 1238-1246

94.   Holford N.H.G., Sheiner L.B. Understanding the dose-effect relationship: Clinical application of pharmacokinetic-pharmacodynamic models. *Clin. Pharmacokinet.* **1981.** 6(6): 429-453

95.   Mager D.E., Wyska E., Jusko W.J. Diversity of mechanism-based pharmacodynamic models. *Drug. Metab. Dispos.* **2003.** 31(5): 510-518

96.   Gabrielsson J., Jusko W.J., Alari L. Modeling of dose-response-time data: Four examples of estimating the turnover parameters and generating kinetic functions from response profiles. *Biopharm. Drug Dispos.* **2000.** 21(2): 41-52

97.   Danhof M., de Jongh J., De lange E.C.M., Della Pasqua O., Ploeger B.A., Voskuyl R.A. Mechanism-based pharmacokinetic-pharmacodynamic modeling: Biophase distribution, receptor theory, and dynamical systems analysis. *Annu. Rev. Pharmacol. Toxicol.* **2007.** 47: 357-400

98.   Rescigno A., Segre G. Drug and tracer kinetics. Blaisdell Publishing Company, London, **1966.**

99.   Yao Z., Krzyzanski W., Jusko W.J. Assessment of basic indirect pharmacodynamic response models with physiological limits. *J. Pharmacokinet. Pharmacodyn.* **2006.** 33(2): 167-193

100.   Peletier L.A., Gabrielsson J. Nonlinear turnover models for systems with physiological limits. *Eur. J. Pharm. Sci.* **2009.** 37(1): 11-26

101.   Licko V., Ekblad E.B.M. Dynamics of a metabolic system: What single-action agents reveal about acid secretion. *Am. J. Physiol.* **1992.** 262(3): 581-592

102.   Sharma A., Ebling W.F., Jusko W.J. Precursor-dependent indirect pharmacodynamic response model for tolerance and rebound phenomena. *J. Pharm. Sci.* **1998.** 87(12): 1577-1584

103.   Ackerman E., Rosevear J.W., McGuckin W.F. A mathematical model of the glucose-tolerance test. *Phys. Med. Biol.* **1964.** 9: 203-213

104.   Wakelkamp M., Alván G., Gabrielsson J., Paintaud G. Pharmacodynamic modeling of furosemide tolerance after multiple intravenous administration. *Clin. Pharmacol. Ther.* **1996.** 60(1): 75-88

105.   Zuideveld K.P., Maas H.J., Treijtel N., Hulshof J., van der Graaf P.H., Peletier L.A., Danhof M. A set-point model with oscillatory behavior predicts the time course of 8-OH-DPAT-induced hypothermia. *Am. J. Physiol. Regul. Integr. Comp. Physiol.* **2001.** 281(6): 2059-2071

106.   Bundgaard C., Larsen F., Jorgensen M., Gabrielsson J. Mechanistic model of acute autoinhibitory feedback action after administration of SSRIs in rats: Application to escitalopram-induced effects on brain serotonin levels. *Eur. J. Pharm. Sci.* **2006.** 29(5): 209-219

107.   Gabrielsson J., Peletier L.A. A flexible nonlinear feedback system that captures diverse patterns of adaptation and rebound. *AAPS. J.* **2008.** 10(1): 70-83

108.   Hammarlund M.M., Odlind B., Paalzow L.K. Acute tolerance to furosemide diuresis in humans. Pharmacokinetic-pharmacodynamic modeling. *Journal of Pharmacology & Experimental Therapeutics.* **1985.** 233(2): 447-453

109.   Chow M.J., Ambre J.J., Ruo T.I., Atkinson J., A.J, Bowsher D.J.,
Fischman M.W. Kinetics of cocaine distribution, elimination, and
chronotropic effects. *Clin. Pharmacol. Ther.* **1985.** 38(3): 318-324

110.   Danhof M., Levy G. Kinetics of drug action in disease states. I. Effect
of infusion rate on phenobarbital concentrations in serum, brain and
cerebrospinal fluid of normal rats at onset of loss of righting reflex. *J.
Pharmacol. Exp. Ther.* **1984.** 229(1): 44-50

111.   Hisaoka M., Danhof M., Levy G. Kinetics of drug action in disease
states. VII. Effect of experimental renal dysfunction on the
pharmacodynamics of ethanol in rats. *J. Pharmacol. Exp. Ther.* **1985.**
232(3): 717-721

112.   Hisaoka M., Levy G. Kinetics of drug action in disease states. IX. Effect
of experimental fever on phenobarbital concentrations at onset of
loss of righting reflex in rats. *J. Pharmacol. Exp. Ther.* **1985.** 232(3):
722-724

113.   Ramzan I.M., Levy G. Kinetics of drug action in disease states. XVIII.
Effect of experimental renal failure on the pharmacodynamics of
theophylline-induced seizures in rats. *J. Pharmacol. Exp. Ther.* **1987.**
240(2): 584-588

114.   Wanwimolruk S., Levy G. Kinetics of drug action in disease states. XX.
Effects of acute starvation on the pharmacodynamics of
phenobarbital, ethanol and pentylenetetrazol in rats and effects of
refeeding and diet composition. *J. Pharmacol. Exp. Ther.* **1987.**
242(1): 166-172

115.   Yasuhara M., Levy G. Kinetics of drug action in disease states. XXVII.
Effect of experimental renal failure on the pharmacodynamics of
zoxazolamine and chlorzoxazone. *J. Pharmacol. Exp. Ther.* **1988.**
246(1): 165-169

116.   Klockowski P.M., Levy G. Kinetics of drug action in disease states.
XXV. Effect of experimental hypovolemia on the pharmacodynamics
and pharmacokinetics of desmethyldiazepam. *J. Pharmacol. Exp.
Ther.* **1988.** 245(2): 508-512

117.   Hoffman A., Levy G. Kinetics of drug action in disease states. XLI. Effect of adrenalectomy on the hypnotic activity of phenobarbital, the neurotoxicity of theophylline and pain sensitivity in rats. *J. Pharmacol. Exp. Ther.* **1993.** 264(2): 859-862

118.   Schonfeld G., Felski C., Howald M.A. Characterization of the plasma lipoproteins of the genetically obese hyperlipoproteinemic Zucker fatty rat. *J. Lipid Res.* **1974.** 15(5): 457-464

119.   Shum L., Jusko W.J. Theophylline disposition in obese rats. *J. Pharmacol. Exp. Ther.* **1984.** 228(2): 380-386

120.   Jaber L.A., Ducharme M.P., Halapy H. The effects of obesity on pharmacokinetics and pharmacodynamics of glipizide in patients with non-insulin-dependent diabetes mellitus. *Ther. Drug Monit.* **1996.** 18(1): 6-13

121.   Cheymol G. Effects of obesity on pharmacokinetics: Implications for drug therapy. *Clin. Pharmacokinet.* **2000.** 39(3): 215-231

122.   Cortinez L.I., Anderson B.J., Penna A., Olivares L., Munoz H.R., Holford N.H.G., Struys M.M.R.F., Sepulveda P. Influence of obesity on propofol pharmacokinetics: derivation of a pharmacokinetic model. *Br. J. Anaesth.* **2010.** 105(4): 448-456

123.   Hanley M.J., Abernethy D.R., Greenblatt D.J. Effect of obesity on the pharmacokinetics of drugs in humans. *Clin. Pharmacokinet.* **2010.** 49(2): 71-87

124.   Stralfors P., Bjorgell P., Belfrage P. Hormonal regulation of hormone-sensitive lipase in intact adipocytes: Identification of phosphorylated sites and effects on the phosphorylation by lipolytic hormones and insulin. *Proc. Natl. Acad. Sci. U. S. A.* **1984.** 81(11): 3317-3321

125.   Frayn K.N., Shadid S., Hamlani R., Humphreys S.M., Clark M.L., Fielding B.A., Boland O., Coppack S.W. Regulation of fatty acid movement in human adipose tissue in the postabsorptive-to-postprandial transition. *Am. J. Physiol. Endocrinol. Metab.* **1994.** 266(3): 308-317

126.   Sadur C.N., Eckel R.H. Insulin stimulation of adipose tissue lipoprotein lipase. Use of the euglycemic clamp technique. *J. Clin. Invest.* **1982.** 69(5): 1119-1125

127.   Zucker L., Zucker T. Fatty, a new mutation in the rat. *J. Hered.* **1961.** 52: 275-278

128.   Zucker L.M., Antoniades H.N. Insulin and obesity in the Zucker genetically obese rat "fatty". *Endocrinology.* **1972.** 90(5): 1320-1330

129.   Bray G.A. The Zucker-fatty rat: a review. *Fed. Proc.* **1977.** 36(2): 148-153

130.   Iwaki M., Ogiso T., Hayashi H., Tanino T., Benet L.Z. Acute dose-dependent disposition studies of nicotinic acid in rats. *Drug. Metab. Dispos.* **1996.** 24(7): 773-779

131.   Sheiner L.B., Beal S.L. Evaluation of methods for estimating population pharmacokinetics parameters. I. Michaelis-Menten model: routine clinical pharmacokinetic data. *J. Pharmacokinet. Biopharm.* **1980.** 8(6): 553-571

132.   Sheiner L.B. The population approach to pharmacokinetic data analysis: rationale and standard data analysis methods. *Drug Metab. Rev.* **1984.** 15(1-2): 153-171

133.   Levy G. Relationship between rate of elimination of tubocurarine and rate of decline of its pharmacological activity. *Br. J. Anaesth.* **1964.** 36: 694-695

134.   Levy G. Kinetics of pharmacologic activity of succinylcholine in man. *J. Pharm. Sci.* **1967.** 56(12): 1687-1688

135.   Gibaldi M., Levy G. Dose-dependent decline of pharmacologic effects of drugs with linear pharmacokinetic characteristics. *J. Pharm. Sci.* **1972.** 61(4): 567-569

136.   Smolen V.F. Quantitative determination of drug bioavailability and biokinetic behavior from pharmacological data for ophthalmic and oral administrations of a mydriatic drug. *J. Pharm. Sci.* **1971.** 60(3): 354-365

137. Verotta D., Sheiner L.B. Semiparametric analysis of non-steady-state pharmacodynamic data. *J. Pharmacokinet. Biopharm.* **1991.** 19(6): 691-712

138. Bragg P., Fisher D.M., Shi J., Donati F., Meistelman C., Lau M., Sheiner L.B. Comparison of twitch depression of the adductor pollicis and the respiratory muscles: Pharmacodynamic modeling without plasma concentrations. *Anesthesiology.* **1994.** 80(2): 310-319

139. Fisher D.M., Wright P.M.C. Are plasma concentration values necessary for pharmacodynamic modeling of muscle relaxants?. *Anesthesiology.* **1997.** 86(3): 567-575

140. Jacqmin P., Snoeck E., van Schaick E.A., Gieschke R., Pillai P., Steimer J.L., Girard P. Modelling response time profiles in the absence of drug concentrations: Definition and performance evaluation of the K-PD model. *J. Pharmacokinet. Pharmacodyn.* **2007.** 34(1): 57-85

141. Kato R. Drug metabolism under pathological and abnormal physiological states in animals and man. *Xenobiotica.* **1977.** 7: 25-92

142. Levy G. Pharmacokinetics in renal disease. *Am. J. Med.* **1977.** 62(4): 461-465

143. Breimer D.D. Pharmacokinetics in liver disease. *Pharm. Weekbl. Sci. Ed.* **1987.** 9(2): 79-84

144. Frayn K.N., Williams C.M., Arner P. Are increased plasma non-esterified fatty acid concentrations a risk marker for coronary heart disease and other chronic diseases? *Clin. Sci.* **1996.** 90(4): 243-253

145. Rowland M., Tozer N.T. Clinical Pharmacokinetics, Concepts and Applications. 3rd ed. Lippincott Williams & Wilkins, Philadelphia, **2009.**

146. Carballo-Jane E., Gerckens L.S., Luell S., Parlapiano A.S., Wolff M., Colletti S.L., Tata J.R., Taggart A.K., Waters M.G., Richman J.G., McCann M.E., Forrest M.J. Comparison of rat and dog models of vasodilatation and lipolysis for the calculation of a therapeutic index for GPR109A agonists. *J. Pharmacol. Toxicol. Methods.* **2007.** 56(3): 308-316

147. Sun Y.N., Jusko W.J. Transit compartments versus gamma distribution function to model signal transduction processes in pharmacodynamics. *J. Pharm. Sci.* **1998.** 87(6): 732-737

148. Savic R.M., Jonker D.M., Kerbusch T., Karlsson M.O. Implementation of a transit compartment model for describing drug absorption in pharmacokinetic studies. *J. Pharmacokinet. Pharmacodyn.* **2007.** 34(5): 711-726

149. Ge H., Li X., Weiszmann J., Wang P., Baribault H., Chen J., Tian H., Li Y. Activation of G protein-coupled receptor 43 in adipocytes leads to inhibition of lipolysis and suppression of plasma free fatty acids. *Endocrinology.* **2008.** 149(9): 4519-4526

150. Bauer J.A., Fung H.L. Differential hemodynamic effects and tolerance properties of nitroglycerin and an S-nitrosothiol in experimental heart failure. *J. Pharmacol. Exp. Ther.* **1991.** 256(1): 249-254

151. Triggle D.J. Desensitization. *Trends Pharmacol. Sci.* **1980.** 1(2): 395-398

152. Guyton A.C. Blood pressure control - Special role of the kidneys and body fluids. *Science.* **1991.** 252(5014): 1813-1816

153. Metcalfe P., Johnston D.G., Nosadini R. Metabolic effects of acute and prolonged growth hormone excess in normal and insulin-deficient man. *Diabetologia.* **1981.** 20(2): 123-128

154. Gill A., Johnston D.G., Orskov H. Metabolic interactions of glucagon and cortisol in man - Studies with somatostatin. *Metab. Clin. Exp.* **1982.** 31(4): 305-311

155. Mittelman S.D., Bergman R.N. Inhibition of lipolysis causes suppression of endogenous glucose production independent of changes in insulin. *Am. J. Physiol.* **2000.** 279(3): 630-637

156. Havel R.J., Carlson L.A., Ekelund L.G., Holmgren A. Studies on the relation between mobilization of free fatty acids and energy metabolism in man: effects of norepinephrine and nicotinic acid. *Metab. Clin. Exp.* **1964.** 13: 1402-1412

157.   Pereira J.N. The plasma free fatty acid rebound induced by nicotinic acid. *J. Lipid Res.* **1967.** 8(3): 239-244

158.   Fuccella L.M., Goldaniga G., Lovisolo P. Inhibition of lipolysis by nicotinic acid and by acipimox. *Clin. Pharmacol. Ther.* **1980.** 28(6): 790-795

159.   Terrettaz J., Assimacopoulos-Jeannet F., Jeanrenaud B. Severe hepatic and peripheral insulin resistance as evidenced by euglycemic clamps in genetically obese fa/fa rats. *Endocrinology.* **1986.** 118(2): 674-678

160.   Goldsmith G.A.M.D., Cordill S.B.A. The vasodilating effects of nicotinic acid: relation to metabolic rate and body temperature. *Am. J. Med. Sci.* **1943.** 205(2): 204-208

161.   Hiatt J.G., Shamsie S.G., Schectman G. Discontinuation rates of cholesterol-lowering medications: Implications for primary care. *Am. J. Manag. Care.* **1999.** 5(4): 437-444

162.   Benyo Z., Gille A., Kero J., Csiky M., Suchankova M.C., Nusing R.M., Moers A., Pfeffer K., Offermanns S. GPR109A (PUMA-G/HM74A) mediates nicotinic acid-induced flushing. *Journal of Clinical Investigation.* **2005.** 115(12): 3634-3640

163.   Pike N.B. Flushing out the role of GPR109A (HM74A) in the clinical efficacy of nicotinic acid. *J. Clin. Invest.* **2005.** 115(12): 3400-3403

164.   Bodor E.T., Offermanns S. Nicotinic acid: An old drug with a promising future. *Br. J. Pharmacol.* **2008.** 153(1): 68-75

165.   Ploeger B.A., Holford N.H.G. Washout and delayed start designs for identifying disease modifying effects in slowly progressive diseases using disease progression analysis. *Pharm. Stat.* **2009.** 8(3): 225-238